The Effect of Heat Treatment on Residual Stress and Machining Distortions in Advanced Nickel Base Disk Alloys

John Gayda
Glenn Research Center, Cleveland, Ohio

Since its founding, NASA has been dedicated to the advancement of aeronautics and space science. The NASA Scientific and Technical Information (STI) Program Office plays a key part in helping NASA maintain this important role.

The NASA STI Program Office is operated by Langley Research Center, the Lead Center for NASA's scientific and technical information. The NASA STI Program Office provides access to the NASA STI Database, the largest collection of aeronautical and space science STI in the world. The Program Office is also NASA's institutional mechanism for disseminating the results of its research and development activities. These results are published by NASA in the NASA STI Report Series, which includes the following report types:

- TECHNICAL PUBLICATION. Reports of completed research or a major significant phase of research that present the results of NASA programs and include extensive data or theoretical analysis. Includes compilations of significant scientific and technical data and information deemed to be of continuing reference value. NASA's counterpart of peer-reviewed formal professional papers but has less stringent limitations on manuscript length and extent of graphic presentations.

- TECHNICAL MEMORANDUM. Scientific and technical findings that are preliminary or of specialized interest, e.g., quick release reports, working papers, and bibliographies that contain minimal annotation. Does not contain extensive analysis.

- CONTRACTOR REPORT. Scientific and technical findings by NASA-sponsored contractors and grantees.

- CONFERENCE PUBLICATION. Collected papers from scientific and technical conferences, symposia, seminars, or other meetings sponsored or cosponsored by NASA.

- SPECIAL PUBLICATION. Scientific, technical, or historical information from NASA programs, projects, and missions, often concerned with subjects having substantial public interest.

- TECHNICAL TRANSLATION. English-language translations of foreign scientific and technical material pertinent to NASA's mission.

Specialized services that complement the STI Program Office's diverse offerings include creating custom thesauri, building customized data bases, organizing and publishing research results . . . even providing videos.

For more information about the NASA STI Program Office, see the following:

- Access the NASA STI Program Home Page at *http://www.sti.nasa.gov*

- E-mail your question via the Internet to help@sti.nasa.gov

- Fax your question to the NASA Access Help Desk at 301–621–0134

- Telephone the NASA Access Help Desk at 301–621–0390

- Write to:
  NASA Access Help Desk
  NASA Center for AeroSpace Information
  7121 Standard Drive
  Hanover, MD 21076

The Effect of Heat Treatment on Residual Stress and Machining Distortions in Advanced Nickel Base Disk Alloys

John Gayda
Glenn Research Center, Cleveland, Ohio

January 2001

Available from

THE EFFECT OF HEAT TREATMENT ON RESIDUAL STRESS AND MACHINING DISTORTIONS IN ADVANCED NICKEL BASE DISK ALLOYS

John Gayda
NASA Glenn Research Center
Cleveland, Ohio

INTRODUCTION

Next generation disk alloys developed under NASA's HSR Program have demonstrated enhanced temperature capability, but this has also made control of residual stress and subsequent machining distortions more challenging. To study these issues NASA's AST and IDPAT Programs (Ref. 1 & 2) initiated tasks to study residual stress and machining distortions in advanced disk alloys. In the AST Program, stabilization heat treatments to minimize residual stresses were developed, while the IDPAT Program developed a methodology to predict machining distortions in nickel base disk alloys. At the end of the IDPAT Program, the methodology for predicting machining distortions was fully developed. However, verification had produced limited success between experimental and analytical results for complex forgings.

This paper describes an extension of the AST and IDPAT Programs, which seeks to predict the effect of heat treatment on residual stress and subsequent machining distortions of simple forgings. Pancake shaped disks of an advanced disk alloy, ME209, were forged and given various heat treatments to produce differing residual stress levels. This was followed by simple face cuts on one side of the disks and measurement of the subsequent distortions on the opposing face. The distortion data were then compared with analytical results based on modeling technology developed in the IDPAT Program.

MATERIAL & PROCEDURES

Four pancake shaped forgings of disk alloy ME209, weighing about 100 pounds each, were isoforged at Wyman-Gordon's R&D Press in Houston using mults cut from a 9" diameter extrusion procured under NASA's AST Program (Ref. 3). Before heat treatment, a bore hole, 0.8" diameter, was added and each forging was also "squared" to yield a pancake shape 14" diameter by 1.9" thick. The four forgings were then given different heat treatments as outlined in Table I. The first three heat treatments produce a fine grain microstructure as a result of the subsolvus solution temperature, 2075F, and were designed to yield progressively lower residual stress levels: as-quenched, quenched and aged at 1400F, and quenched and stabilized at 1550F. The fourth heat treatment produces a coarse grain microstructure as a result of the supersolvus solution temperature, 2160F, and was included to provide a direct comparison with the subsolvus, stabilized heat treatment. After heat treatment, a small groove was cut in the side of the forgings as shown in Figure 1. The groove and bore hole would serve as clamping points for subsequent machining operations.

At this point, the four forgings were measured to obtain the initial distortion/warpage resulting from forging and/or heat treatment. The in-plane distortion was characterized by

measuring the vertical deviation from an imaginary circle of 1" radius at the center of a forging per the layout presented in Figure 2. As seen in that sketch, 48 points were used to characterize the warpage on the bottom side of each forging. The measurements were made using a Sheffield Cordax CMM System with a spatial resolution of 0.001". In addition thickness measurements were made at 0, 90, 180, and 270° along an imaginary circle of 6" radius.

The first of two face cuts were made on the top surface of each forging as shown in Figure 1. The first cut went to a depth of 0.24", while the second cut went an additional 0.24" for a total depth of 0.48". These face cuts were made on a 36" Monarch Engine Lathe using a Kennametal carbide cutting tool (KC950 Grade/RNMG64 Insert) with a water-based coolant. The lathe ran at a constant speed of 67RPM and utilized a feed of 0.010"/revolution. Multiple passes averaging about 0.030" cutting depth were used to make each of the two face cuts. To minimize movement during cutting, the forgings were clamped to a large steel base utilizing two C-shaped clamps in the side groove and a bolt at the bore hole, as seen in Figure 3. The entire assembly is then inserted into a four jaw chuck on the lathe. In between each cut, the forgings were removed so that warpage and thickness measurements could be made on the bottom surface using the same methodology described in the preceding paragraph.

Residual stresses were modeled using a finite element method for each of the four heat treatments in this study. The analysis provided a complete picture of the stress distribution in the forgings, which is required for predicting part deflection after each machining operation. To calculate residual stresses, a commercial finite element package from Algor was employed with the appropriate approximations of thermal and mechanical properties for ME209. A complete discussion of the properties will be presented in the next section of this paper. The first step in the analysis involves construction of a 2-D axisymmetric model of the forgings. The finite element model and mesh are shown in Figure 4. Before the stresses can be calculated, a transient thermal analysis must be run to simulate each of the four heat treatments in this study. The output from this analysis is used to drive a viscoplastic stress analysis that generates the residual stress state at the end of each heat treatment. To simulate the machining operations and predict the resulting distortions, the modulus of elements to be "machined" are reduced to negligible, i.e. near zero, levels. Comparison between experimental and analytical distortions can then be made to verify the model.

RESULTS & DISCUSSION

The results of the distortion measurements before and after machining are summarized in tabular form in the Appendix for each of the four heat treatments. Examination of the data revealed several trends. First, the in-plane warpage of the disks was somewhat surprising. As seen in Figure 5, the disks had an irregular in-plane warp along the hoop direction (warp versus angle). While the in-plane warp in the hoop direction was irregular, this did not result from variations in initial thickness (thick versus angle), see Figure 5. Further, the irregular pattern of the in-plane warp persisted even after the machining operations, as shown in Figure 6, but the change in mean level at any particular point was remarkably consistent for each cut. The consistency of the change in

distortion upon machining is even more evident on examining the warpage maps along the radial direction, Figure 7.

As a result of the irregular nature of the initial warp in the disks, it was felt that the subsequent analysis of the data would be simplified if the change in distortion was tracked and modeled. To this end, a comparison of the experimentally measured changes in distortion of the two face cuts are summarized in Figure 8, for the four heat treatments. Specifically, the average rim deflection at the 6" radial location (final value-initial value) is plotted as a function of heat treatment and depth of cut. As one can see, the trend was as expected for the subsolvus heat treatments, and not surprisingly the comparison between the supersolvus and subsolvus heat treatments given the 1550F stabilization show that the supersolvus solution yields higher distortion levels and therefore less stress relief for a given stabilization treatment.

Before modeling of the distortion could be attempted, estimates of the thermal, physical, and mechanical properties of ME209 were required. Most of the data was obtained from the AST Program (Ref. 3). For the thermal analysis, values for conductivity, density, and specific heat were readily available and are summarized in Table II. However, precise values for the heat transfer coefficient, h, were not available. Estimates of h were obtained from a calibration forging of similar dimensions utilized in the AST Regional Disk Program (Ref. 4). Analysis of that forging indicated the best fit to h during the quench after the solution heat treatment was obtained using an $h=0.3BTU/(IN^2-HR-F)$ during the transfer from the furnace to the quench tank and an $h=1.3BTU/(IN^2-HR-F)$ in the oil. While the choice of constant h during the quench, both spatially and temporally, is somewhat inaccurate, lack of data and limitations of the Algor FEA software necessitated this choice. On heating and cooling during subsequent ages at 1400 and 1550F an $h=0.2BTU/(IN^2-HR-F)$ was employed. The mechanical properties used in the viscoplastic stress analysis were functions of temperature and are summarized in Tables III and IV for the subsolvus and supersolvus heat treatments respectively. Most of the entries in these tables are self-explanatory, however, the last two columns require some explanation. These data represent the coefficient and exponent in a power-law creep expression. They were obtained by simulating actual stress relaxation tests on ME209 at 1400 and 1550F with a one element FEA model. Results of the simulation at 1550F for the subsolvus material and actual relaxation data are presented in Figure 9. Comparing the data in Tables III and IV it should be noted that the supersolvus heat treatment is characterized by somewhat lower yield strengths at lower temperatures, but significantly higher creep resistance.

With the aforementioned thermal properties, the four heat treatments were simulated with a transient thermal analysis using the FEA model/mesh in Figure 4. The most critical portion of the analysis is the simulation of the oil quench. As seen in Figure 10, significant thermal gradients are produced in the forging after a short time in the oil. These gradients die out after 15 minutes, Figure 11, and the part is essentially at the oil temperature, which was assumed to be 100F for this study. Subsequent heating and cooling of the part during stabilization and aging generates much smaller gradients, Figure 12, as h is much smaller, 0.2 versus $1.3BTU/(IN^2-HR-F)$, and their impact is

relatively minor. However, the extended exposure at temperature will have a significant impact on residual stresses as significant relaxation can occur during these extended periods.

Having completed the thermal analyses, the viscoplastic stress analyses can now be run and the resulting residual stress distributions examined. As the resulting analyses produce a multiaxial stress distribution many plots are available for viewing, however, the hoop stresses are dominant and provide the most information at a glance. Starting with the subsolvus oil quench, Figure 13 shows the stress state at 0.02 hours into the quench, when a significant portion of the forging is still quite hot, see Figure 10, while Figure 14 shows the stress state at the end of the quench, when the part temperature is essentially 100F. Note the reversal of the stress sign between the part interior and exterior at these two times. Initially the exterior is in tension as it cools much faster than the interior. With the rapid cooling rate produced by the oil quench, the forging yields and this produces a non-reversible path which puts the exterior in compression when the forging reaches room temperature. If plastic flow does not occur on cooling, the stresses vanish as the part temperature equilibrates. Supersolvus oil quenching, Figure 15, produces a similar stress distribution although the peak stresses are somewhat higher. This is to be expected as the solution temperature is 85F higher for the supersolvus heat treatment. Subsequent aging and/or stabilization alter the residual stress distributions. As one might expect, they drop the peak stress levels over that observed for the as-quenched condition. Their impact is directly related to the degree of stress relaxation that can occur during the extended period at the age and/or stabilization temperature. As previously stated, the effect of heating and cooling during this portion of a heat treat cycle is relatively minor. This is a direct result of the limited thermal gradient produced in the part on heating and/or cooling. Although the stresses are observed to rise as the thermal gradient increases with heating or cooling, the magnitude is generally insufficient to cause significant plastic flow, and when the part reaches thermal equilibrium, the stresses generally return to their original value. With this information in mind, one can now compare the changes in the residual stress distributions for the 1400F age, Figure 16, and the 1550F stabilization, Figures 17 and 18. Examination of these distributions reveal the 1550F stabilization have a far greater impact than the 1400F age, and the 1550F stabilization treatment has more impact on material with a fine grain microstructure (subsolvus) than that with a coarse grain microstructure (supersolvus). This ranking is rational and consistent with the relaxation data presented in Figure 19. One last observation worth noting, is the 1400F age cycle had little impact on the residual stress distributions following the 1550F stabilization. This occurs as the peak stress levels after stabilization are far below the stresses observed in the relaxation data shown in Figure 19. In other words, exposure at 1400F, following stabilization at 1550F, would require times far in excess of eight hours to have any significant impact on the residual stress distributions after stabilization.

With the residual stress distributions available, the distortions for each of the two face cuts can now be modeled. As previously stated, this is done by reducing the modulus of "machined" elements to negligible levels. Starting with the oil quenched forging one can see the first face cut produces significant distortion, Figure 20. In this figure, the "machined" elements have been hidden and the displacements have been magnified by a

factor of ten for clarity. Also the shape of the undeflected part is shown for reference. This analysis was repeated for the other heat treatments as well as the second face cut. The results of these analyses are compared with the experimental data in Figures 21 and 22. In these plots, the average rim deflection, at the 6" radial location, are compared. One can see the analytical results track the experimental data quite well. Both experimental and analytical results confirm that the 1550F/3HR stabilization treatment is an effective stress relief cycle for fine grain (subsolvus) ME209. However, coarse grain (supersolvus) ME209 obviously requires longer stabilization times or higher stabilization temperatures to achieve the same degree of stress relief obtained for fine grain ME209.

Several observations about the analysis and use of FEA modeling should be made at this point. First, these experimental data clearly validate the analytical approach developed under the IDPAT Program, however, several issues of technological importance require further study. Initial distortions resulting from forging/heat treatment can be modeled provided one has reliable estimates describing the variation of the heat transfer coefficient, h, along the parts perimeter. In this study that data was not available and, in general, is hard to obtain experimentally (Ref. 5). Continued development and accurate verification of CFD based estimates for h would be extremely useful in this respect. Second, the interaction of the forging, clamping, and tooling during the machining process must be included in the FEA modeling if one hopes to use this approach to guide the development of efficient machining plans for complex disk shapes. In this study this factor was not important, as dimensional data was always taken from the bottom surface of the forging while all machining was restricted to the top surface. Finally, a more detailed understanding of microstructural evolution during heat treatment is probably warranted. Since microstructure evolves during the heat treatment process, mechanical properties are also changing and therefore the material properties in the FEA model should not be fixed, but vary continually to reflect reality. Efforts to predict this evolution (Ref. 6) and include its effect in the FEA model should be studied.

SUMMARY & CONSLUSIONS

This paper describes an extension of the AST and IDPAT Programs which sought to predict the effect of stabilization heat treatments on residual stress and subsequent machining distortions in the advanced disk alloy, ME-209. Simple "pancake" forgings of ME-209 were produced and given four heat treatments:

2075F(SUBSOLVUS)/OIL QUENCH/NO AGE
2075F/OIL QUENCH/1400F@8HR
2075F/OIL QUENCH/1550F@3HR/1400F@8HR
2160F(SUPERSOLVUS)/OIL QUENCH/1550F@3HR/1400F@8HR

The forgings were then measured to obtain surface profiles in the heat treated condition. A simple machining plan consisting of face cuts from the top surface followed by measurements of the surface profile opposite the cut were made. This data provided warpage maps which were compared with analytical results. The analysis followed the IDPAT methodology and utilized a 2-D axisymmetric, viscoplastic FEA code. The

analytical results accurately tracked the experimental data for each of the four heat treatments. The 1550F stabilization heat treatment was found to significantly reduce residual stresses and subsequent machining distortions for fine grain (subsolvus) ME209, while coarse grain (supersolvus) ME209 would require additional time or higher stabilization temperatures to attain the same degree of stress relief.

While the current study certainly validated the IDPAT methodology for predicting machining distortions, several issues/areas were identified that could enhance predictive capability. They included CFD based estimates of the heat transfer coefficient, interaction of the forging with clamping fixtures and tooling, and refined estimates of material properties which "evolve" during the heat treat process.

REFERENCES

1. P.L. Reynolds, "High OPR Core Materials AOI 4.2.6 Effects of Residual Stress Heat Treatments", Final Report, NASA Contract NAS3-27720, November 1999.
2. D.G. Backman, E.S. Russell, K. Singh, and D.Y. Wei, "Integrated Design and Processing Analysis Technology", Final Report, NASA Contract NAS3-26617, December 1998.
3. J.C. Chesnutt, R.G. Tolbert, and D.P. Mourer, "High OPR Core Materials AOI 4.2.5 Forging Process Definition of Alloy 2", Final Report, NASA Contract NAS3-27720, November 1999.
4. S.K. Jain, "High OPR Core Materials AOI 4.2.4 Regional Engine Disk Development", Final Report, NASA Contract NAS3-27720, November 1999.
5. R.W. Bass, "Heat Transfer of Turbine Disks in Liquid Quench", Final Report, NASA Contract NAS3-97039, December 1998.
6. T.P. Gabb, D.G. Backman, D.Y. Wei, D.P. Mourer, D. Furrer, A. Garg, and D.L. Ellis, "Gamma Prime Formation in a Nickel-Base Disk Superalloy", Superalloys 2000, TMS Publication, pp.405-414, September 2000.

TABLE I. HEAT TREATMENTS.

PRE-HEAT TREAT MACHINING: 14"DIA X 1.9"THICK WITH 0.8" DIA BORE HOLE						
GENTLE RADIUS ON ALL EDGES						
FORGING		HEAT TREATMENT				
2	2075F/2HR/OIL QUENCH					
3	2075F/2HR/OIL QUENCH + 1400F/8HR					
4	2075F/2HR/OIL QUENCH + 1550F/3HR + 1400F/8HR					
1	2060F/1HR+2160F/1HR/OIL QUENCH + 1550F/3HR + 1400F/8HR					
NOTE: SOLUTION AND QUENCH STEP ON 2,3, & 4 SHOULD BE IDENTICAL						

TABLE II. THERMAL PROPERTIES.

Index	Temperature	Kn	Ks	Kt	Specific Heat
1	0	0.4	0.4	0.4	0.10
2	1200	0.9	0.9	0.9	0.12
3	2300	1.3	1.3	1.3	0.23

TABLE III. SUBSOLVUS PROPERTIES.

2-D Viscoplastic Material: [Customer Defined]

Unlock Properties

Mass Density: 0.30 lbf/in²/in/in²

Material Properties versus Temperature Data

Viscoplastic Properties

Temperature	Modulus	Poisson's	Hardening	Yield	Thermal Coefficient	1st	2nd Coefficient
0	30E6	.30	1000	160E3	7E-6	0	4
1300	27E6	.30	1000	150E3	8E-6	0	4
1500	24E6	.35	1000	130E3	9E-6	8E-24	4
1900	20E6	.40	100	20E3	10E-6	40E-22	4
2200	70E5	.45	10	1E3	12E-6	40E-22	4

Add Row   Delete Row   Sort

OK   Cancel   Apply   Print   Reset From Default

TABLE IV. SUPERSOLVUS PROPERTIES.

Material Properties versus Temperature Data

Viscoplastic Properties

Temperature	Modulus	Poisson's	Hardening	Yield	Thermal Coefficient	1st	2nd Coefficient
0	30E6	.30	1000	150E3	7E-6	0	4
1300	27E6	.30	1000	140E3	8E-6	0	4
1500	24E6	.35	1000	120E3	9E-6	4E-24	4
1900	20E6	.40	100	20E3	10E-6	40E-23	4
2300	20E6	.45	10	1E3	13E-6	40E-22	4

FIGURE 1. MACHINING PLAN.

MACHINED REGION

.50 MAX ON FINAL CUT

1.9

12 O'CLOCK REFERENCE HOLE

0.80

.375 R

5.5

MACHINED REGION

7.00

FIGURE 2. MEASUREMENT PLAN.

12 O'CLOCK POSITION

12.5 POINT
(12 O'CLOCK @ 5")

REFERENCE HOLE
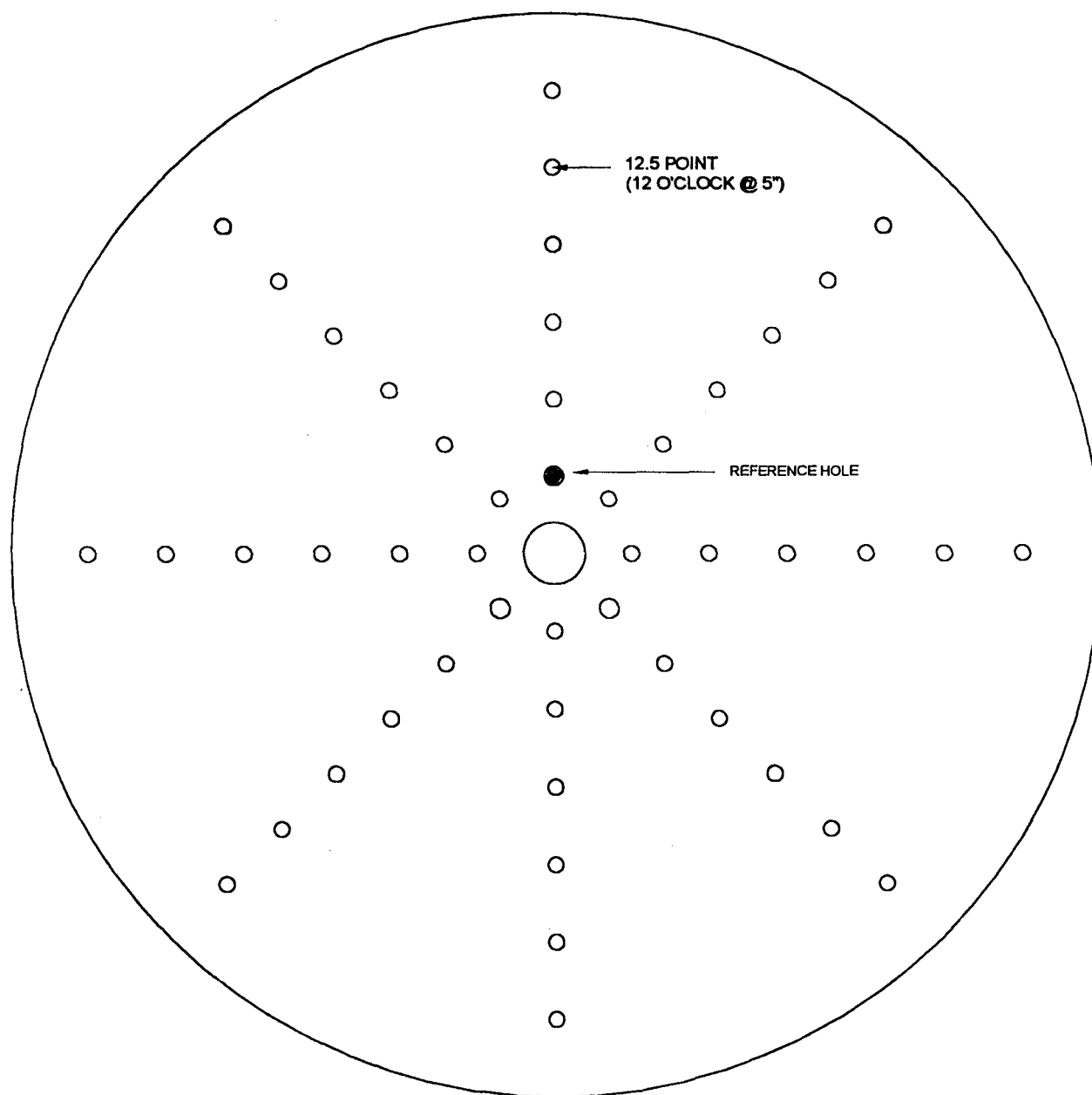
BOTTOM VIEW
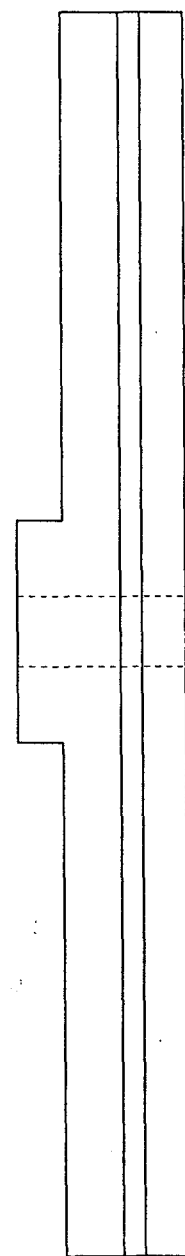
SIDE VIEW

FIGURE 3. MACHINING OF FORGING.
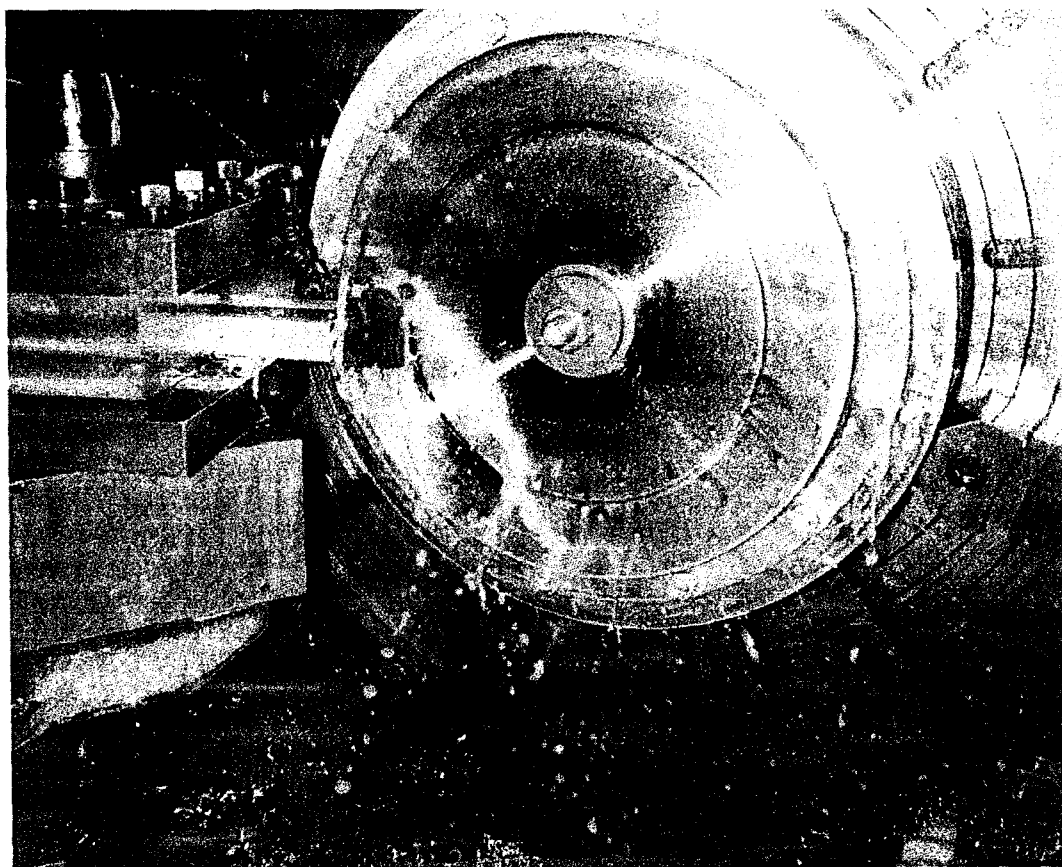
FIGURE 4. FEA MODEL AND MESH.

2D AXISYMMETRIC MODEL OF FORGING

14" DIAMETER X 1.52" THICK WITH 0.8" DIAMETER BORE HOLE
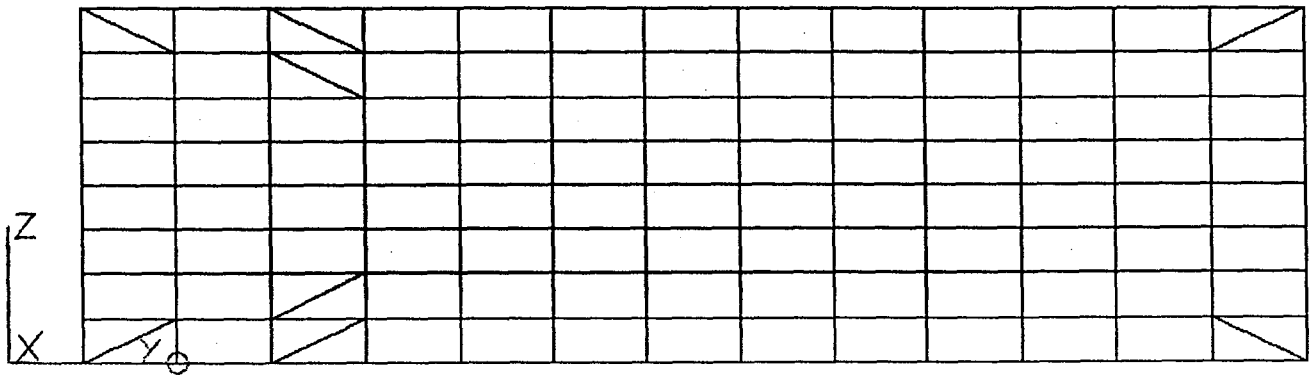
FIGURE 5. INITIAL VARIATION OF IN-PLANE WARPAGE AND THICKNESS.

PART 2 - RUN 1
(R=6")
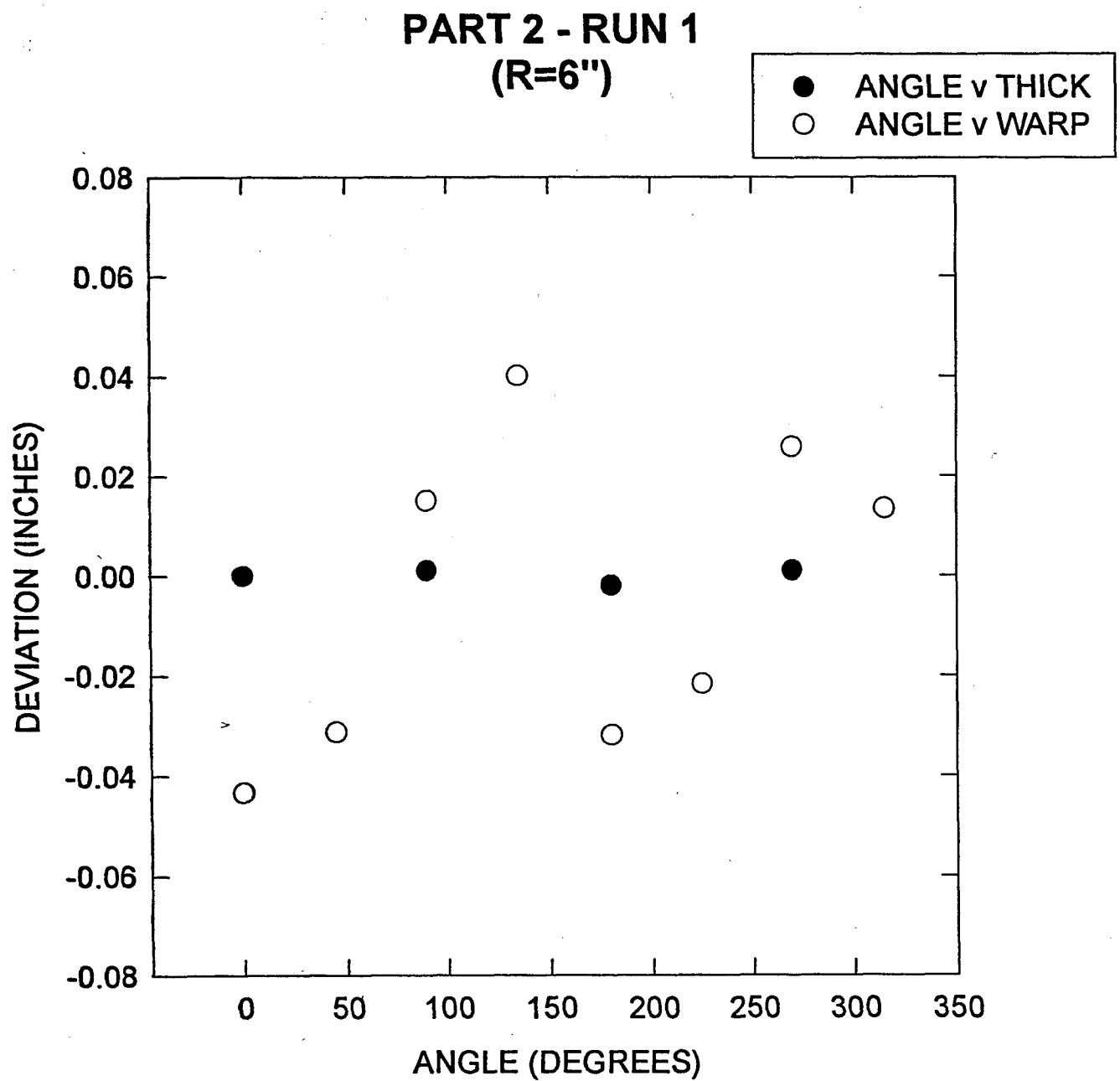
FIGURE 6. COMPARISON OF IN-PLANE WARPAGE BEFORE (RUN 1) AND AFTER FIRST CUT (RUN 2).
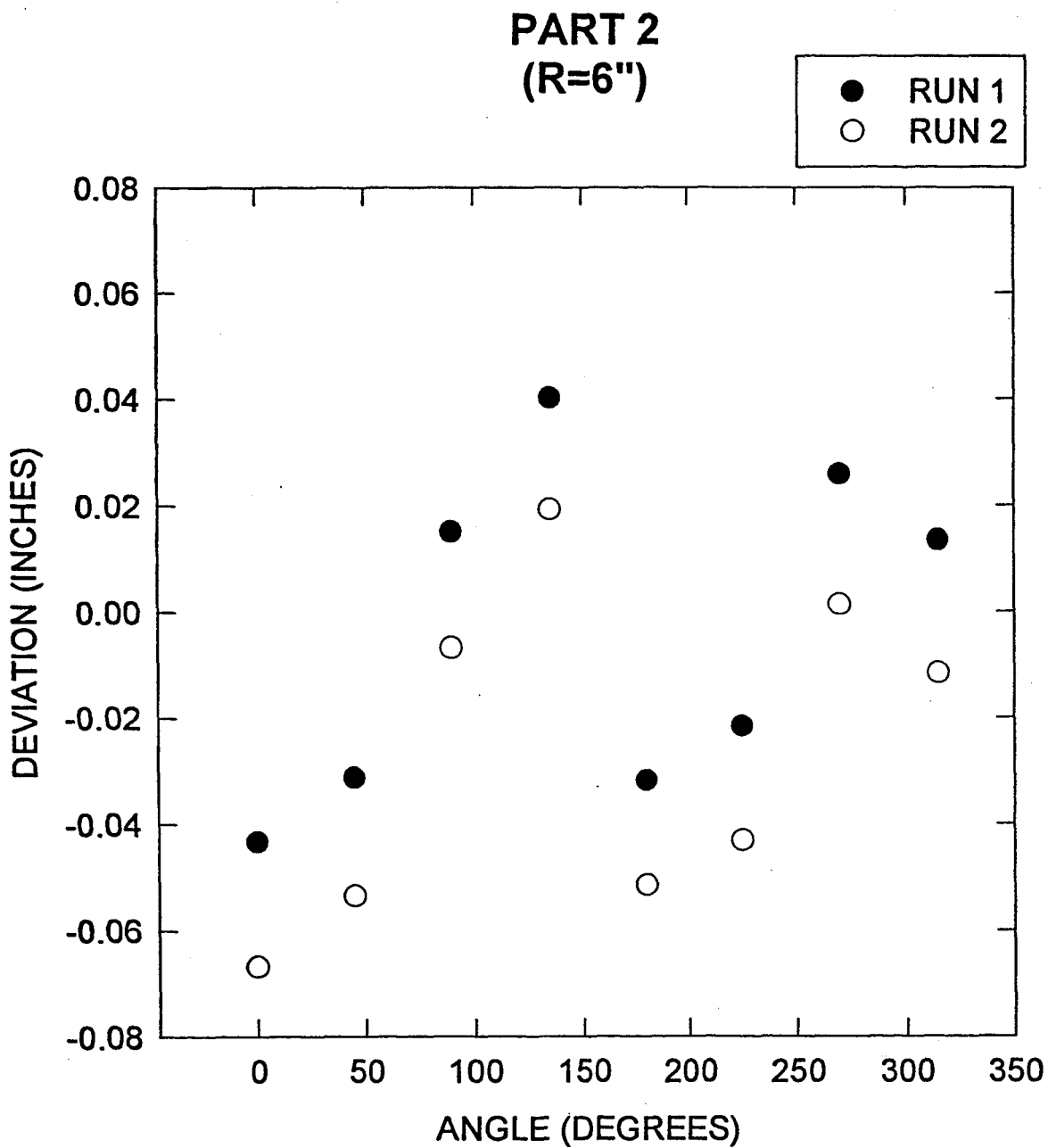
FIGURE 7. CHANGE IN AVERAGE Z(HEIGHT) DEFLECTION AS A FUNCTION OF RADIAL LOCATION.

WARPAGE MAP
PART 2
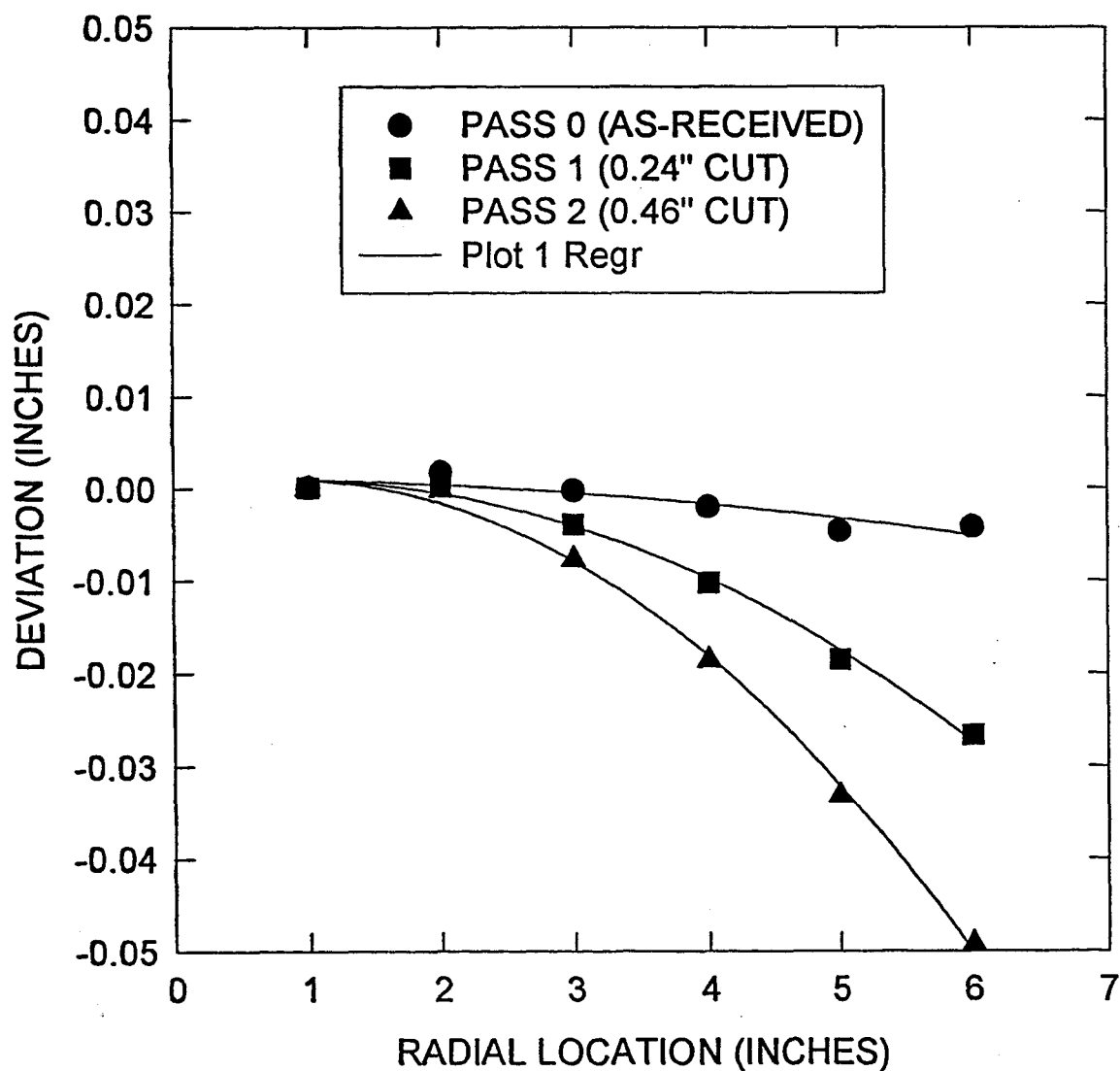
FIGURE 8. COMPARISON OF AVERAGE RIM DEFLECTION AMONG THE FOUR HEAT TREATMENTS.

AVERAGE RIM DEFLECTION AT R=6"
ALLOY ME209
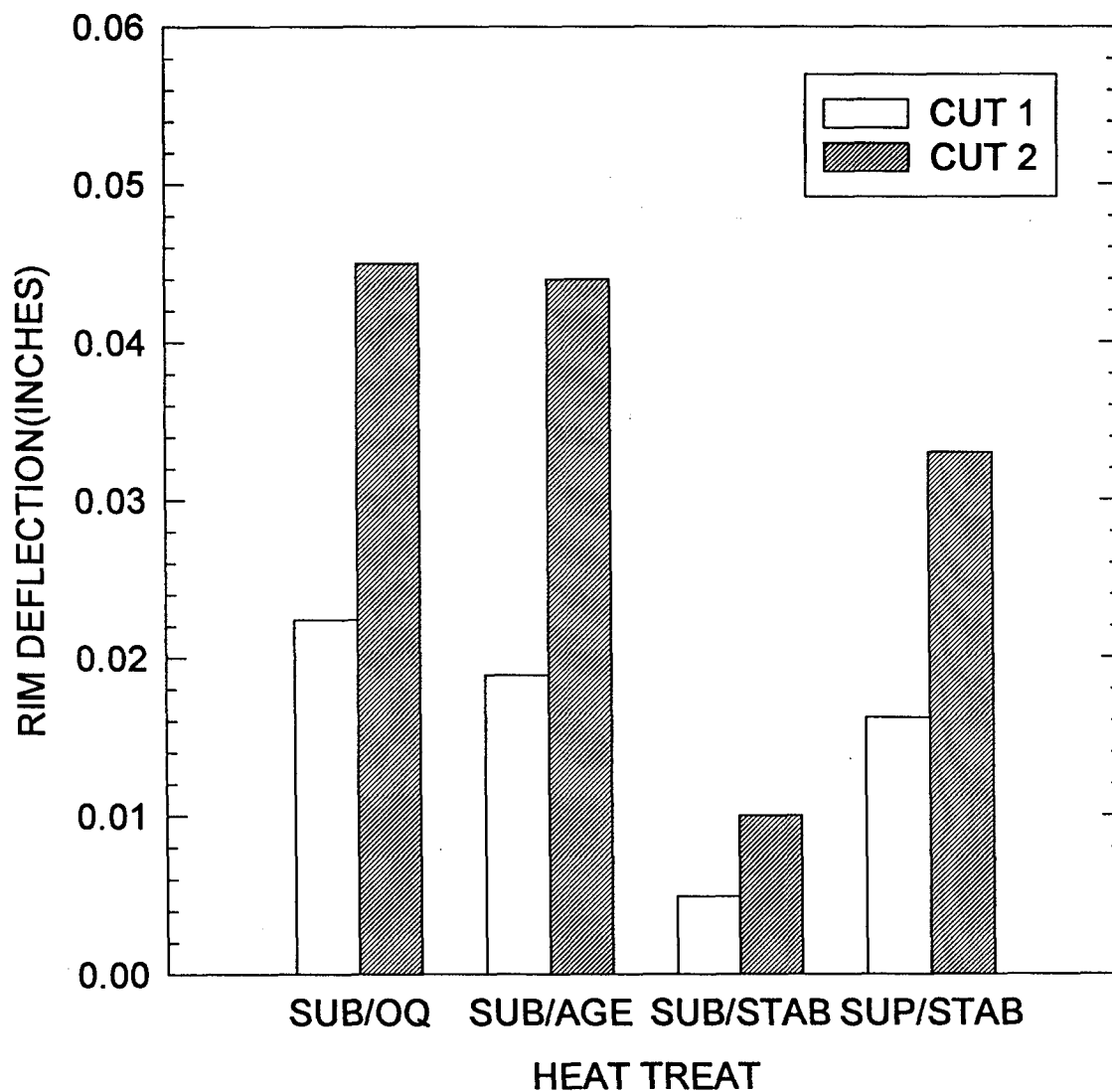
FIGURE 9. COMPARISON OF EXPERIMENTAL AND ANALYTICAL RELAXATION CURVES.

MAX STRESS(PSI) 1550F RELAXATION(SUBSOLVUS)
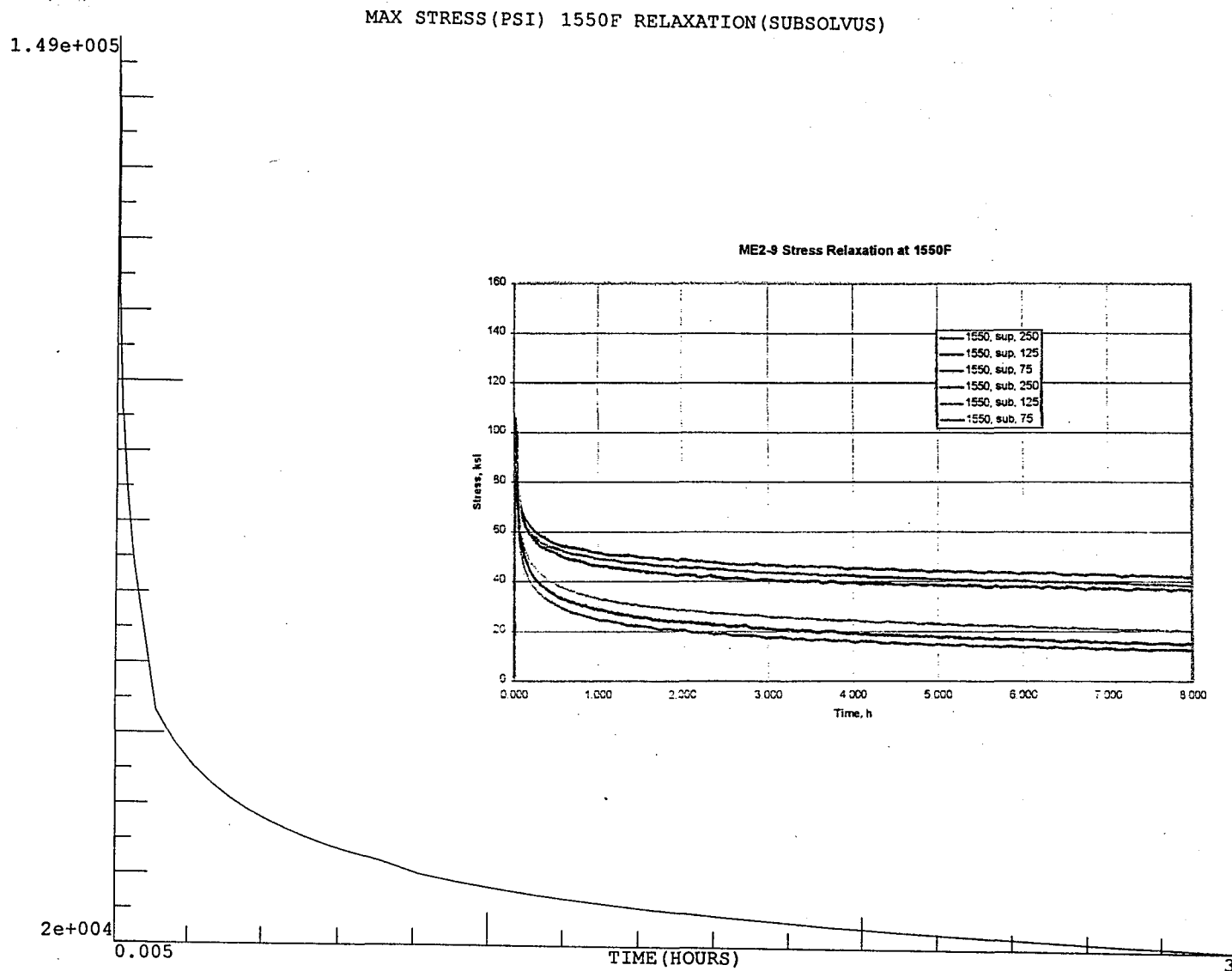
FIGURE 10. TEMPERATURE GRADIENT IN FORGING AT THE ONSET OF QUENCHING.
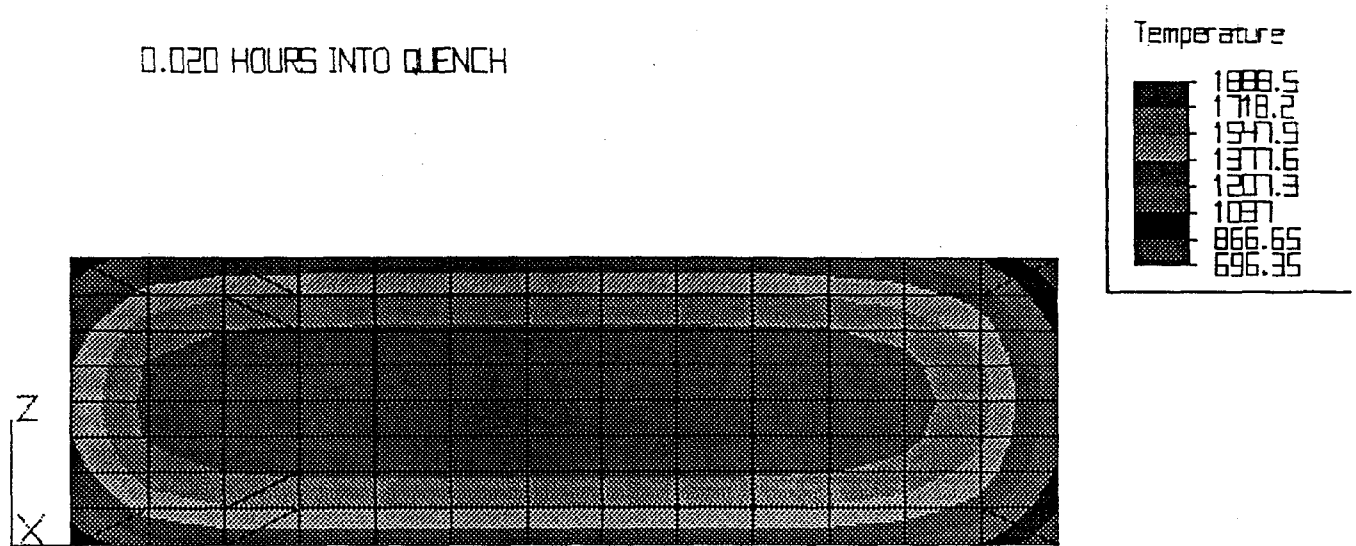
FIGURE 11. VARIATION OF EXTREME NODAL TEMPERATURES DURING THE QUENCH.

HEAT TRANSFER COEFFICIENTS=0.3/1.3

NODES
——— (1).T
············ (64).T
·—·— (126).T
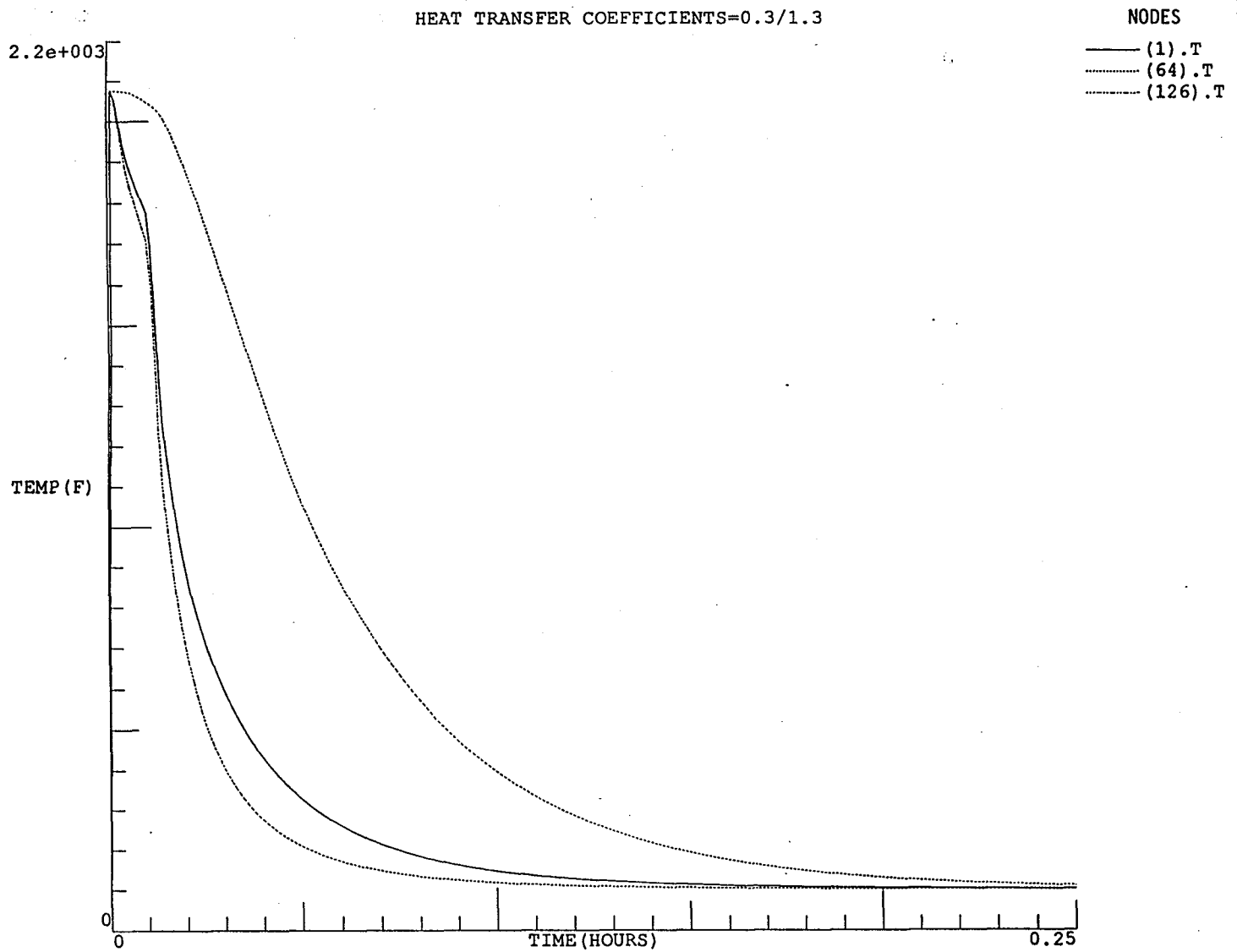
FIGURE 12. VARIATION OF EXTREME NODAL TEMPERATURES DURING THE AGE.

1400F AGE
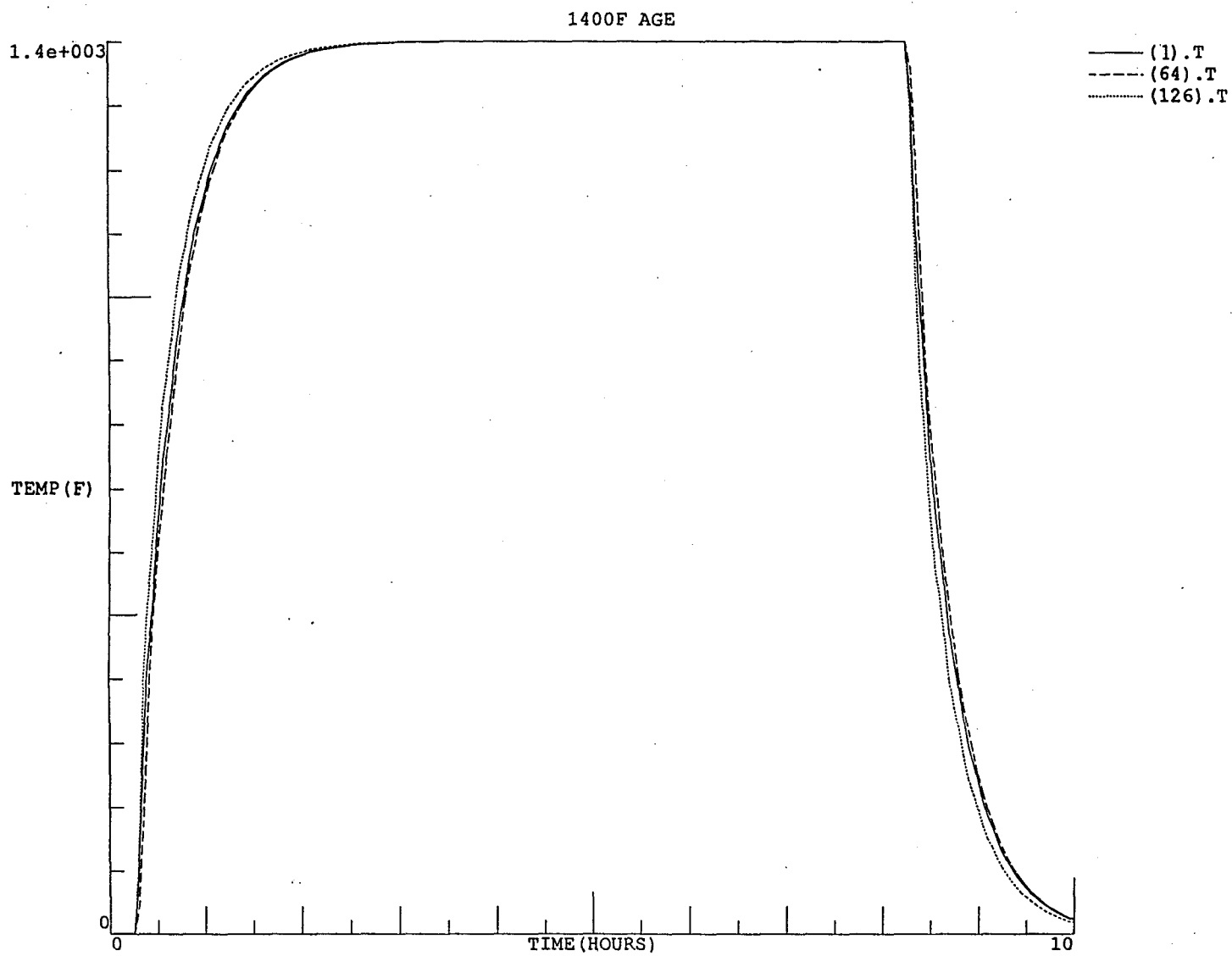
FIGURE 13. HOOP STRESS AT ONSET OF QUENCH. NOTE HIGH TENSILE COMPONENT ON SURFACE BALANCED BY INTERIOR COMPRESSIVE COMPONENT.

HOOP STRESS(PSI)

0.02 HOURS INTO OIL QUENCH

Tensor

259968
211245
162521
113798
65074.6
16351.2
-32372.3
-81095.7
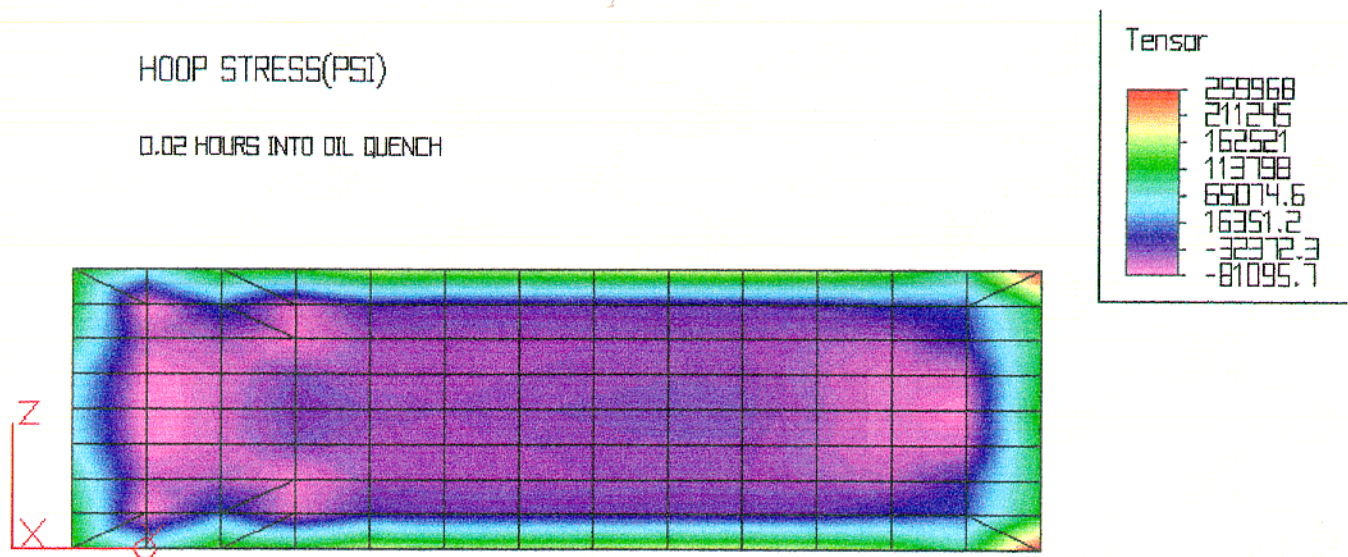
FIGURE 14. HOOP STRESS AT END OF QUENCH. NOTE REVERSAL OF STRESS SIGN FROM THAT SHOWN IN FIGURE 13.

HOOP STRESS(PSI)

OIL QUENCH

Tensor

122825
80316.3
37807
-4702.16
-47211.4
-89720.6
-132230
-174739
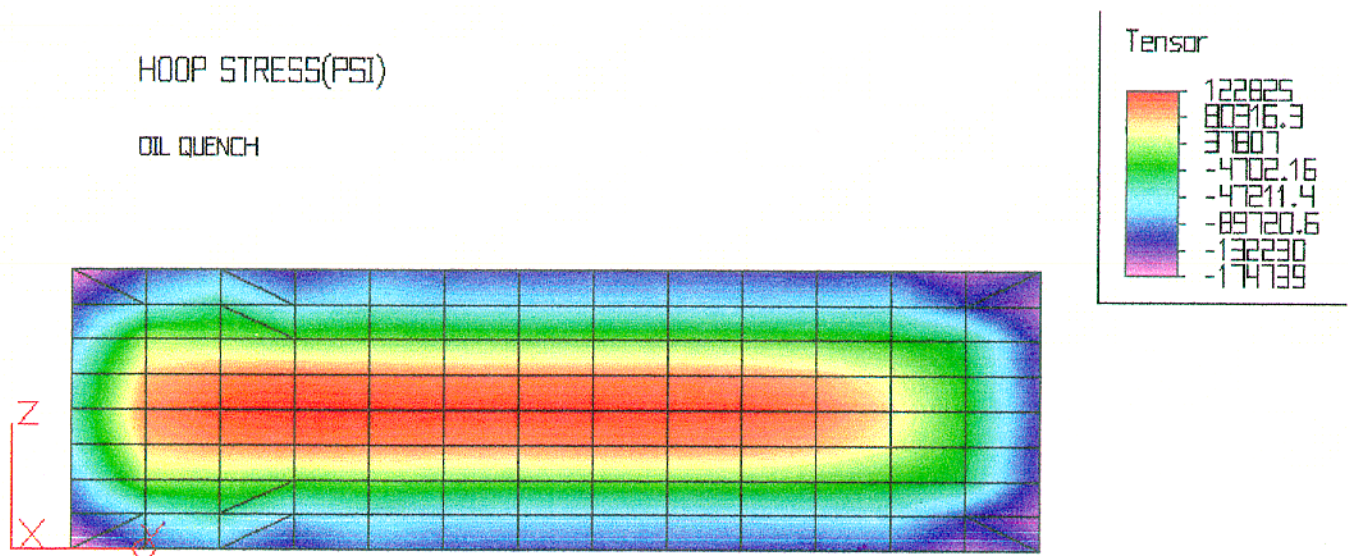
FIGURE 15. HOOP STRESS AT END OF SUPERSOLVUS QUENCH.

HOOP STRESS(PSI)

SUPERSOLVUS QUENCH

Tensor

142146
92353.5
42560.9
-7231.62
-57024.2
-106817
-156609
-206402
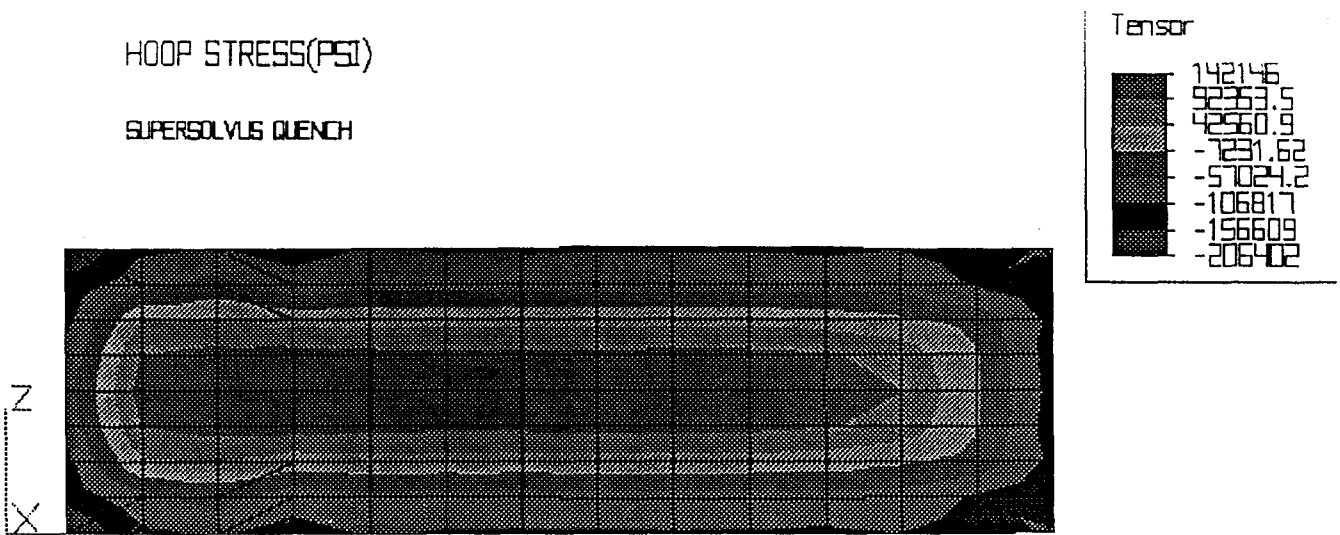
FIGURE 16. HOOP STRESS AT END OF 1400F AGE.

HOOP STRESS(PSI)

1400F AGE

Tensor

86611.4
54547.8
22484.2
-9579.48
-41643
-73706.7
-105770
-137834
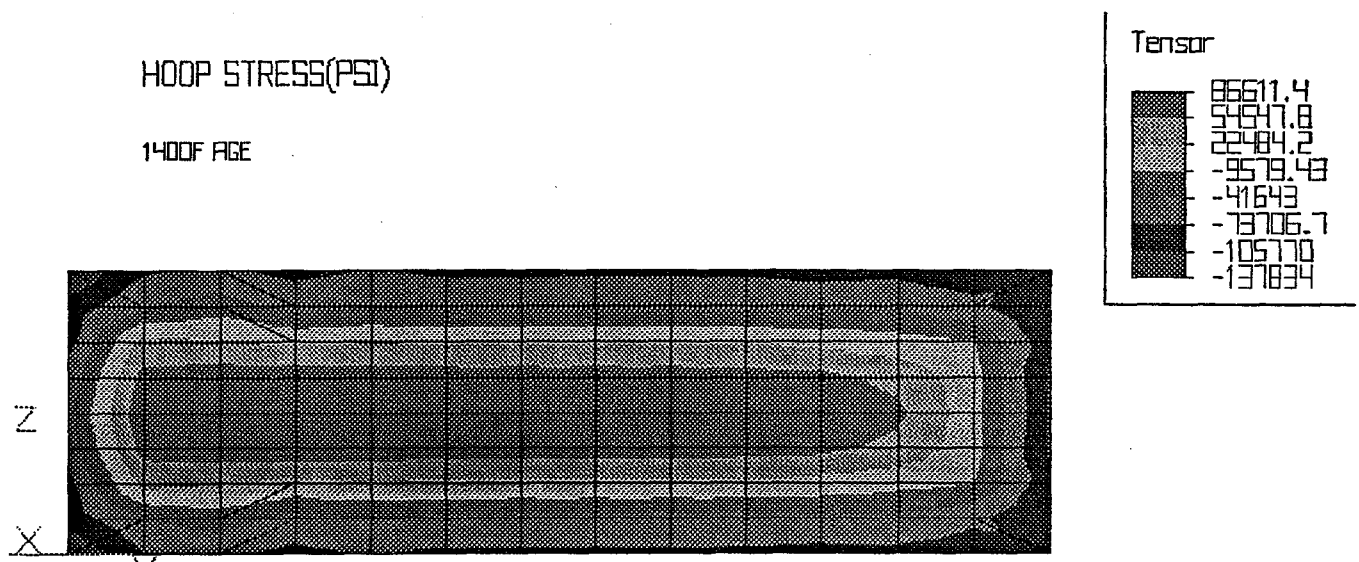
FIGURE 17. HOOP STRESS AT END OF 1550F STABILIZATION FOR SUBSOLVUS MATERIAL.

HOOP STRESS(PSI)

1550F AGE

Tensor

41865
26729
11594
-3541.9
-18677
-33813
-48949
-64084
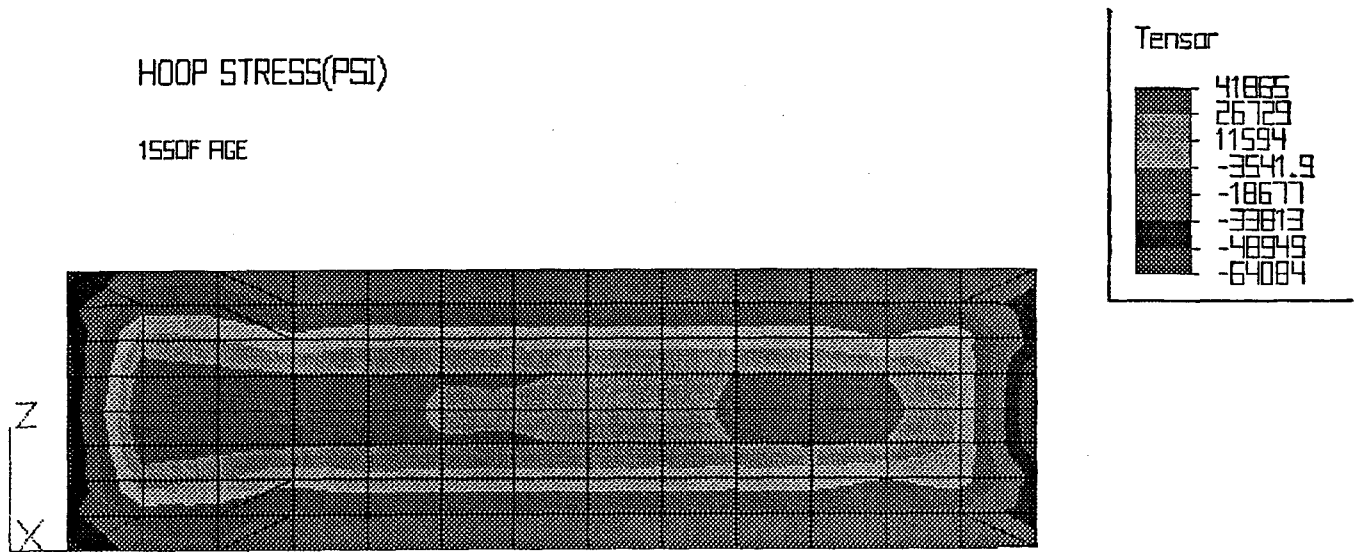
FIGURE 18. HOOP STRESS AT END OF 1550F STABILIZATION FOR SUPERSOLVUS MATERIAL.

HOOP STRESS(PSI)

SUPERSOLVUS 1550F AGE

Tensor

70944.7
45073.1
19201.5
-6670.08
-32541.7
-58413.3
-84284.9
-110156
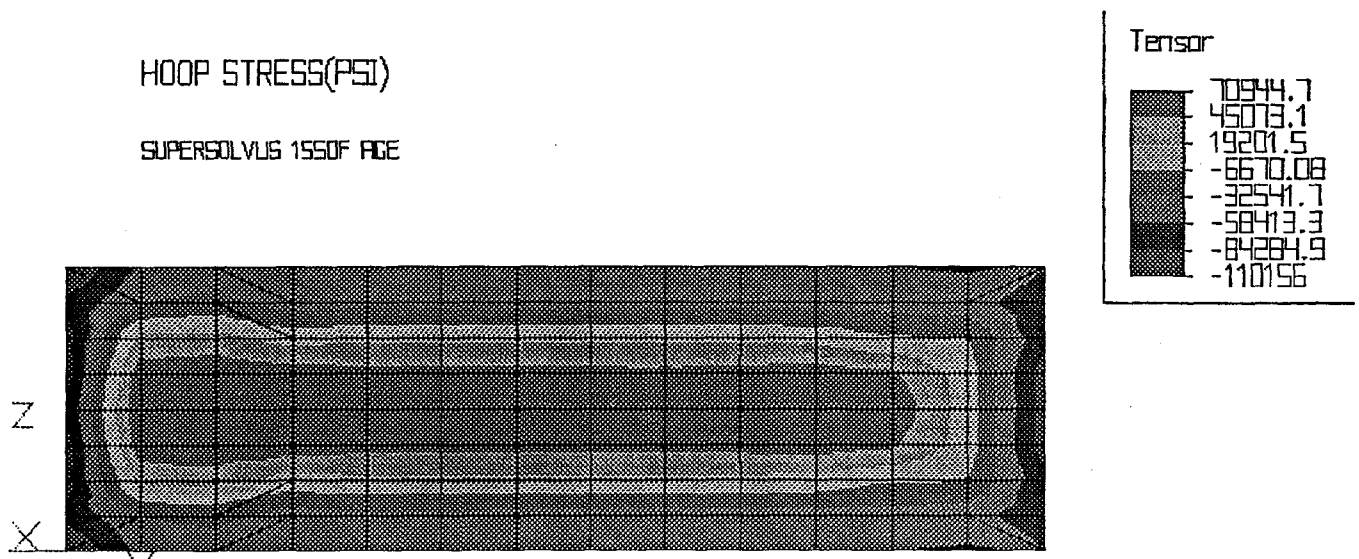
FIGURE 19. RELAXED STRESSES AFTER FOUR HOURS FOR SUBSOLVUS AND SUPERSOLVUS MATERIAL.
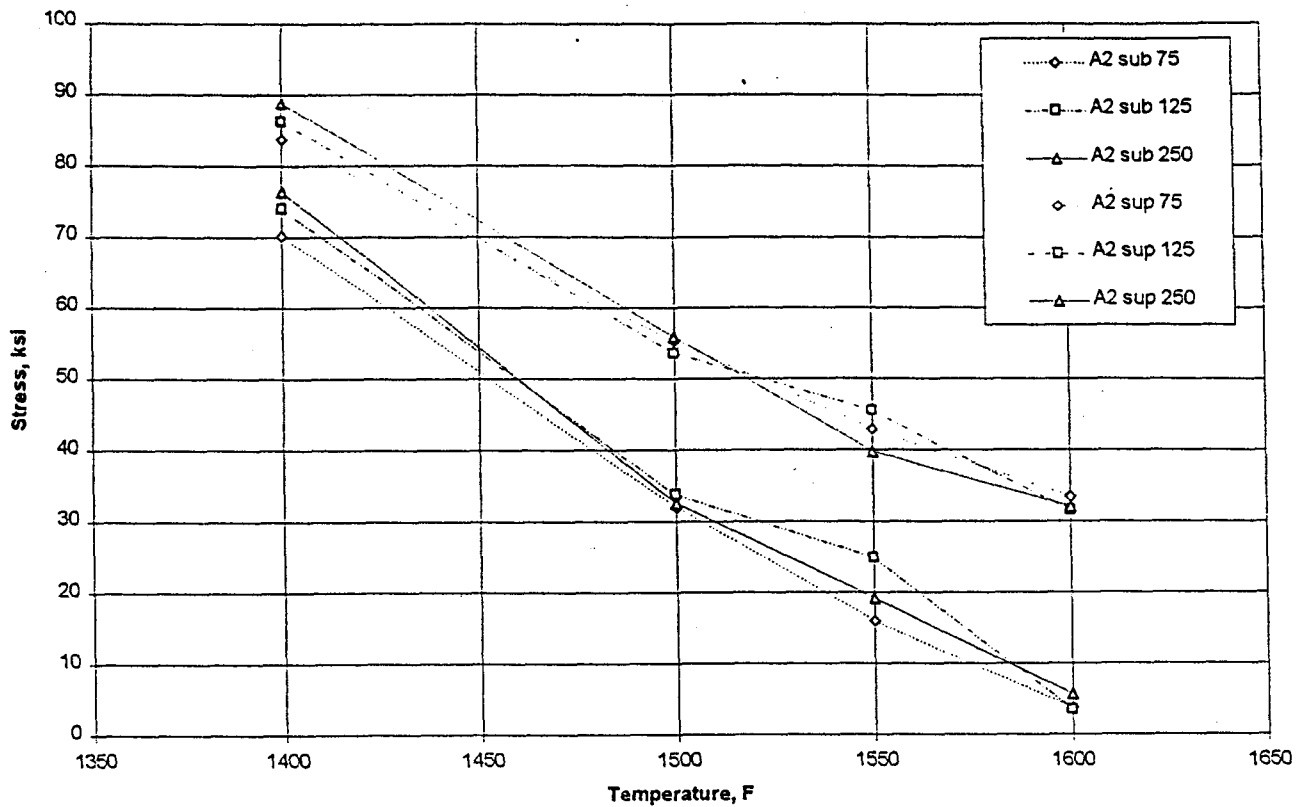
FIGURE 20. FEA DEFLECTION PREDICTION.

Z DISPLACEMENT(INCHES)

DISP MAG=10X

SUBSOLVUS QUENCH (0.24" CUT)

Displacement
- 0.03409
- 0.02878
- 0.02347
- 0.01816
- 0.01284
- 0.00753
- 0.00222
- -0.003
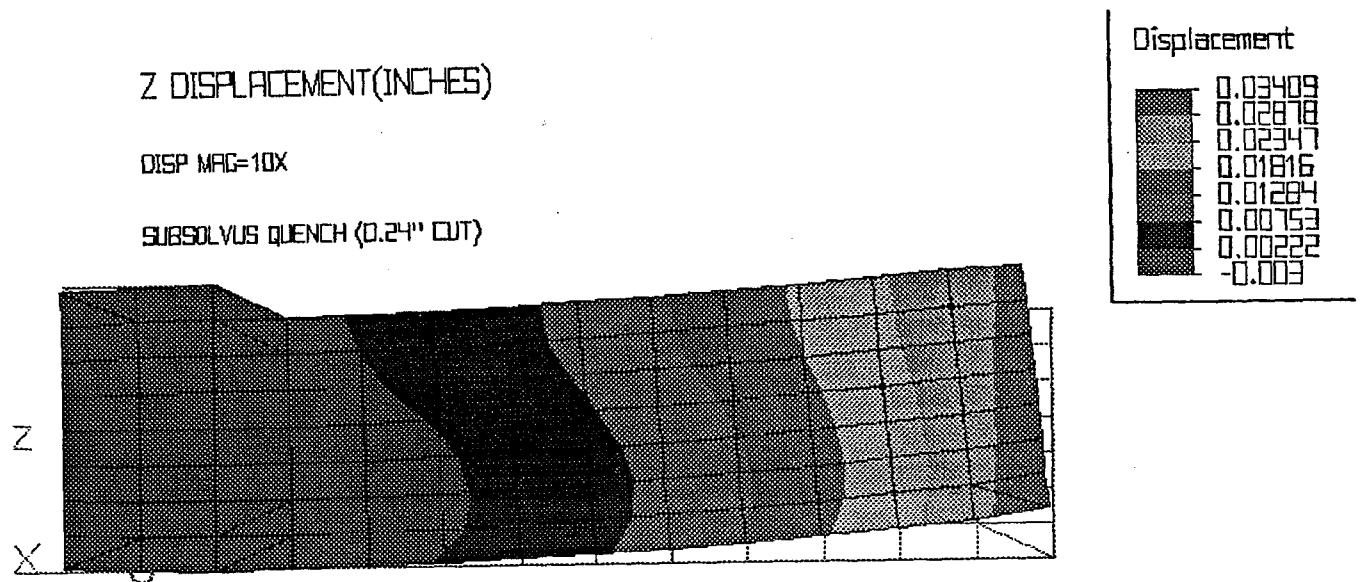
FIGURE 21. COMPARISON OF FEA AND EXPERIMENTAL DEFLECTIONS FOR FIRST CUT (0.24").

AVERAGE RIM DEFLECTION AT R=6" FOR 0.24" CUT
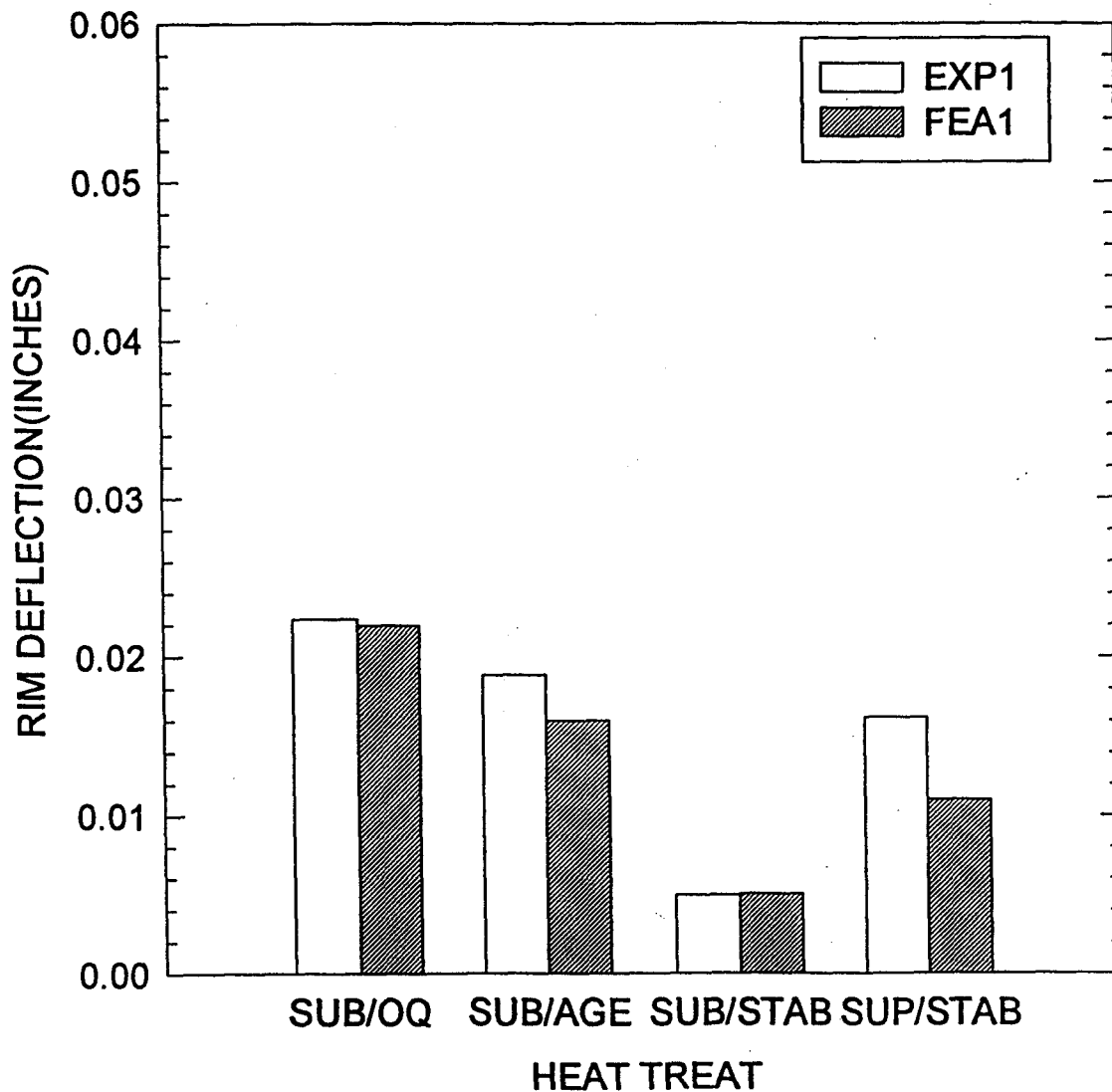
FIGURE 22. COMPARISON OF FEA AND EXPERIMENTAL DEFLECTIONS FOR SECOND CUT (0.48″).
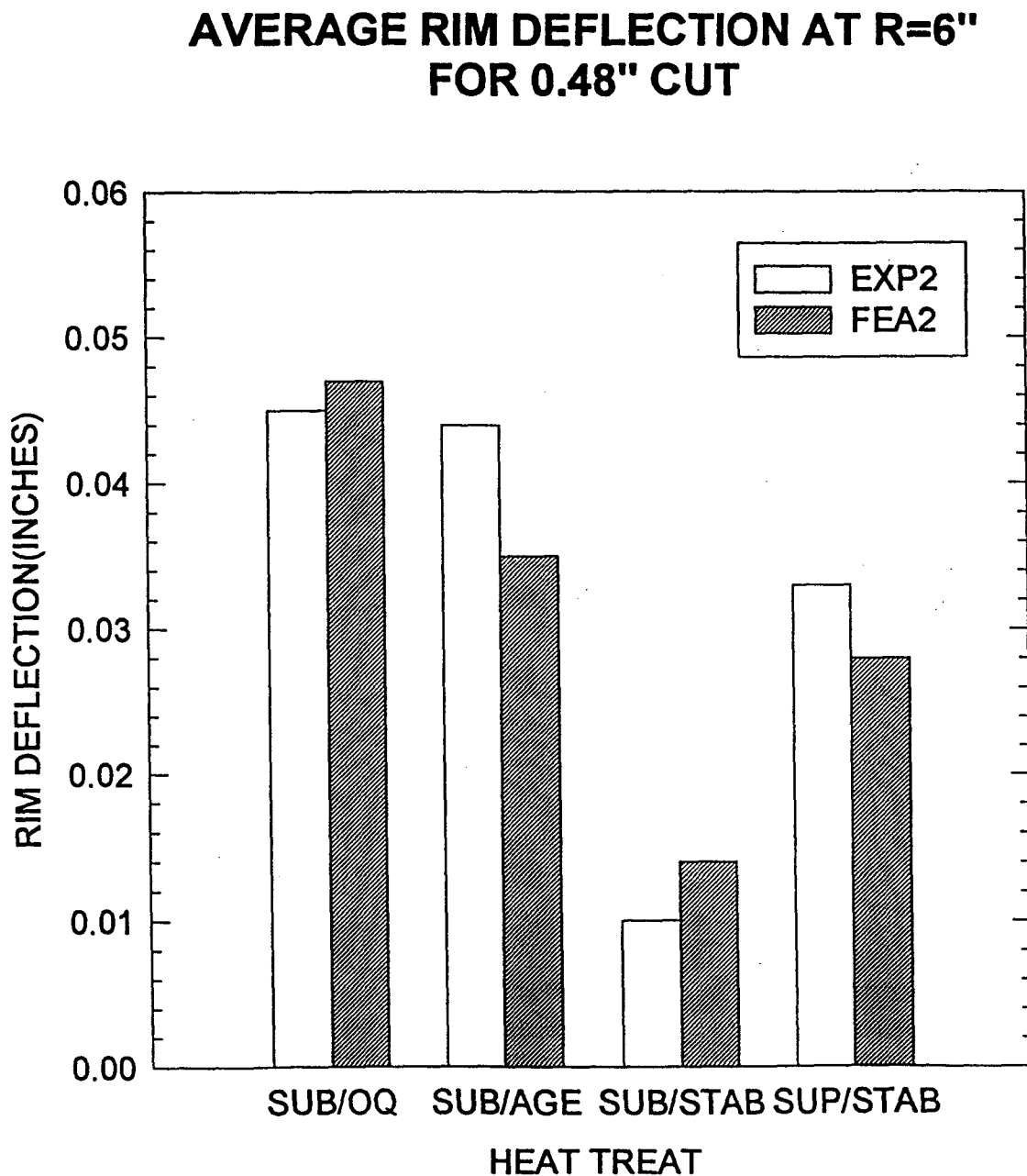
APPENDIX

SUMMARY

| PART | CUT1 | EXPERIMENTAL MACHINING DATA | | | | | | |
		DEF1	CUT2	DEF2	CUTTOT	DEFTOT	HEAT TREAT	RADIUS
1	0.27	0.0162	0.22	0.0164	0.49	0.0326	SUP/STAB	1.4
2	0.24	0.0224	0.22	0.0227	0.46	0.0451	SUB/OQ	1.45
3	0.23	0.0189	0.25	0.0259	0.48	0.0448	SUB/AGE	1.6
4	0.27	0.0049	0.2	0.0049	0.47	0.0098	SUB/STAB	1.35

ANGLE	0	45	90	135	180	225	270	315	AVERAGE
					PART 1 RUN 1				
RADIAL 1	0.0016	0.0001	0.0014	0.0015	-0.0006	0.0004	0.0036	0.0038	0.0015
RADIAL 2	0.0060	0.0037	0.0097	0.0105	0.0022	0.0037	0.0135	0.0135	0.0079
RADIAL 3	0.0072	0.0032	0.0174	0.0213	0.0009	0.0034	0.0235	0.0219	0.0124
RADIAL 4	0.0104	0.0030	0.0284	0.0390	0.0003	0.0024	0.0380	0.0335	0.0194
RADIAL 5	0.0173	0.0045	0.0433	0.0641	0.0024	0.0012	0.0582	0.0489	0.0300
RADIAL 6	0.0172	-0.0002	0.0521	0.1224	-0.0036	-0.0056	0.0756	0.0574	0.0394
NOTE: 12 O'CLOCK @ ANGLE=0 (CCW PROGRESSION)							R.ANG	THICK	
RADIAL 1 @ 1.1" RADIAL 2 THRU 6 @ 2" THRU 6"							6.000	1.920	
RUN 1=AS-RECEIVED							6.090	1.922	
							6.180	1.924	
							6.270	1.910	

ANGLE	0	45	90	PART 1 RUN 2 135	180	225	270	315	AVERAGE
RADIAL 1	0.0011	-0.0003	0.0013	0.0015	0.0000	0.0009	0.0038	0.0039	0.0015
RADIAL 2	0.0045	0.0024	0.0086	0.0101	0.0025	0.0039	0.0129	0.0127	0.0072
RADIAL 3	0.0036	-0.0003	0.0139	0.0188	-0.0004	0.0018	0.0207	0.0187	0.0096
RADIAL 4	0.0034	-0.0039	0.0214	0.0332	-0.0036	-0.0023	0.0317	0.0268	0.0133
RADIAL 5	0.0056	-0.0071	0.0317	0.0537	-0.0056	-0.0078	0.0473	0.0377	0.0194
RADIAL 6	-0.0002	-0.0176	0.0350	0.1066	-0.0167	-0.0203	0.0588	0.0403	0.0232
NOTE: 12 O'CLOCK @ ANGLE=0 (CCW PROGRESSION)							R.ANG	THICK	
RADIAL 1 @ 1.1" RADIAL 2 THRU 6 @ 2" THRU 6"							6.000	1.653	
RUN 2=0.2" NOMINAL CUT							6.090	1.672	
							6.180	1.588	
							6.270	1.676	

ANGLE	0	45	90	135	PART 1 RUN 3 180	225	270	315	AVERAGE
RADIAL 1	0.0009	-0.0005	0.0011	0.0015	-0.0005	0.0003	0.0031	0.0032	0.0011
RADIAL 2	0.0036	0.0016	0.0080	0.0094	0.0014	0.0023	0.0112	0.0114	0.0061
RADIAL 3	0.0005	-0.0033	0.0114	0.0165	-0.0033	-0.0020	0.0168	0.0153	0.0065
RADIAL 4	-0.0032	-0.0106	0.0155	0.0278	-0.0095	-0.0095	0.0246	0.0201	0.0069
RADIAL 5	-0.0054	-0.0184	0.0214	0.0443	-0.0154	-0.0192	0.0358	0.0266	0.0087
RADIAL 6	-0.0172	-0.0350	0.0184	0.0913	-0.0318	-0.0367	0.0418	0.0233	0.0068
NOTE: 12 O'CLOCK @ ANGLE=0 (CCW PROGRESSION)						R.ANG	THICK		
RADIAL 1 @ 1.1" RADIAL 2 THRU 6 @ 2" THRU 6"						6.000	1.446		
RUN 3=0.4" NOMINAL CUT						6.090	1.459		
						6.180	1.358		
						6.270	1.464		

WARPAGE MAP
PART 1
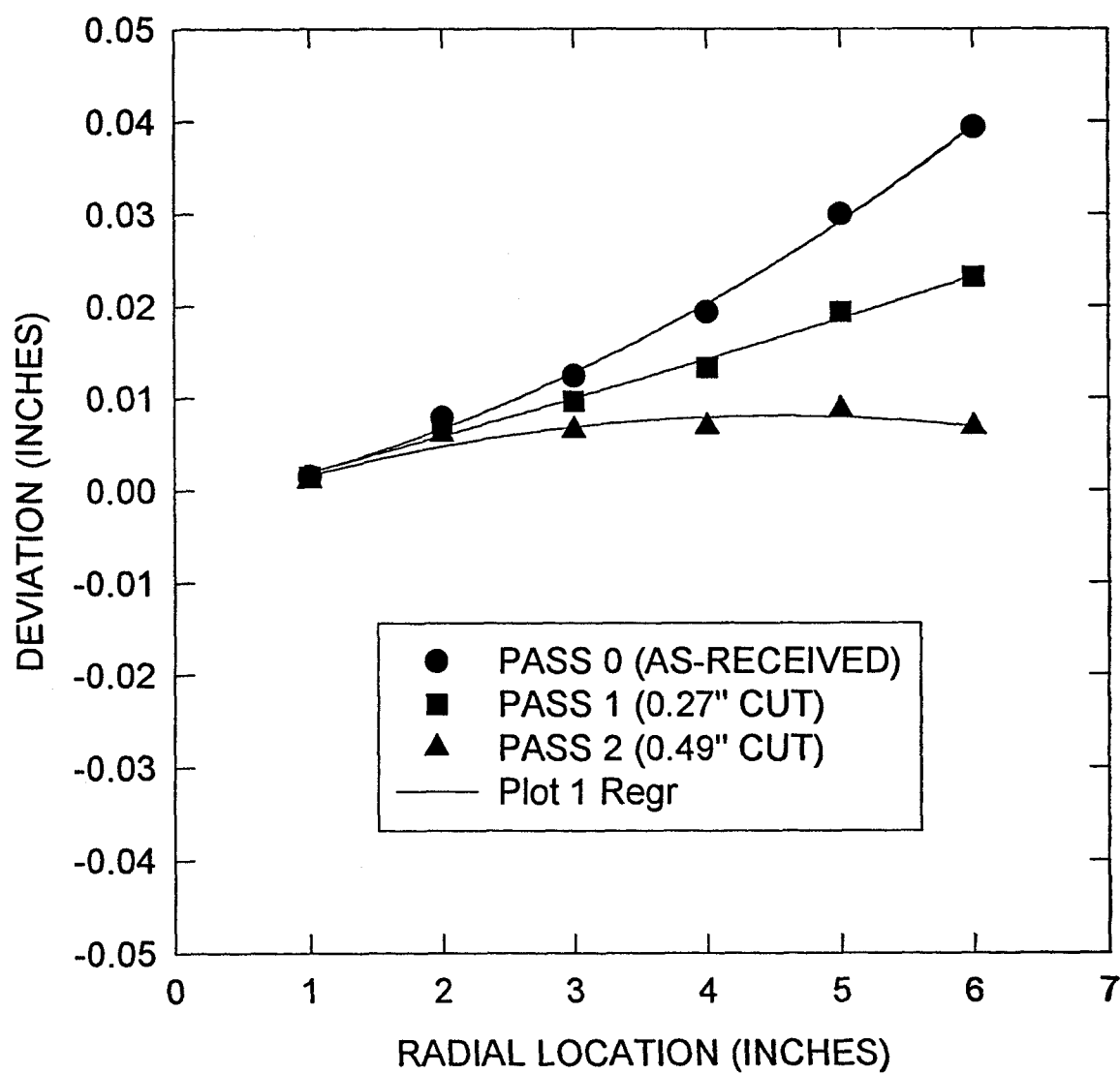
ANGLE	0	45	90	135	180	225	270	315	AVERAGE
					PART 2 RUN 1				
RADIAL 1	-0.0006	-0.0010	-0.0002	-0.0003	-0.0014	-0.0003	0.0025	0.0024	0.0001
RADIAL 2	-0.0029	-0.0031	0.0024	0.0039	-0.0015	0.0014	0.0079	0.0064	0.0018
RADIAL 3	-0.0105	-0.0084	0.0037	0.0037	-0.0067	-0.0012	0.0110	0.0069	-0.0002
RADIAL 4	-0.0193	-0.0139	0.0072	0.0038	-0.0129	-0.0058	0.0158	0.0091	-0.0020
RADIAL 5	-0.0299	-0.0241	0.0120	0.0045	-0.0203	-0.0121	0.0213	0.0119	-0.0046
RADIAL 6	-0.0433	-0.0313	0.0151	0.0402	-0.0319	-0.0217	0.0259	0.0135	-0.0042
							R.ANG	THICK	
NOTE: 12 O'CLOCK @ ANGLE=0 (CCW PROGRESSION)							6.000	1.912	
RADIAL 1 @ 1.1" RADIAL 2 THRU 6 @ 2" THRU 6"							6.090	1.913	
RUN 1=AS-RECEIVED							6.180	1.910	
							6.270	1.913	

ANGLE	0	45	90	PART 2 RUN 2 135	180	225	270	315	AVERAGE
RADIAL 1	-0.0006	-0.0010	-0.0003	-0.0005	-0.0014	-0.0002	0.0025	0.0023	0.0001
RADIAL 2	-0.0036	-0.0040	0.0012	0.0030	-0.0021	0.0005	0.0067	0.0054	0.0009
RADIAL 3	-0.0139	-0.0121	-0.0002	0.0001	-0.0098	-0.0047	0.0069	0.0027	-0.0039
RADIAL 4	-0.0275	-0.0217	-0.0012	-0.0039	-0.0199	-0.0138	0.0068	0.0000	-0.0102
RADIAL 5	-0.0445	-0.0354	-0.0025	-0.0089	-0.0327	-0.0258	0.0056	-0.0041	-0.0185
RADIAL 6	-0.0668	-0.0535	-0.0068	0.0193	-0.0515	-0.0431	0.0014	-0.0117	-0.0266
NOTE: 12 O'CLOCK @ ANGLE=0 (CCW PROGRESSION)							R.ANG	THICK	
RADIAL 1 @ 1.1" RADIAL 2 THRU 6 @ 2" THRU 6"							6.000	1.633	
RUN 2=0.2" NOMINAL CUT							6.090	1.722	
							6.180	1.653	
							6.270	1.675	

ANGLE	0	45	90	135	180	225	270	315	AVERAGE
				PART 2 RUN 3					
RADIAL 1	-0.0014	-0.0018	-0.0006	-0.0004	-0.0009	0.0002	0.0027	0.0021	0.0000
RADIAL 2	-0.0058	-0.0060	0.0000	0.0024	-0.0022	0.0007	0.0064	0.0040	-0.0001
RADIAL 3	-0.0200	-0.0178	-0.0045	-0.0029	-0.0120	-0.0068	0.0040	-0.0017	-0.0077
RADIAL 4	-0.0388	-0.0330	-0.0106	-0.0112	-0.0259	-0.0197	-0.0003	-0.0095	-0.0186
RADIAL 5	-0.0632	-0.0537	-0.0186	-0.0218	-0.0438	-0.0370	-0.0076	-0.0202	-0.0332
RADIAL 6	-0.0944	-0.0809	-0.0316	-0.0014	-0.0695	-0.0611	-0.0194	-0.0364	-0.0493
NOTE: 12 O'CLOCK @ ANGLE=0 (CCW PROGRESSION)							R.ANG	THICK	
RADIAL 1 @ 1.1" RADIAL 2 THRU 6 @ 2" THRU 6"							6.000	1.421	
RUN 3=0.4" NOMINAL CUT							6.090	1.492	
							6.180	1.415	
							6.270	1.454	

WARPAGE MAP
PART 2
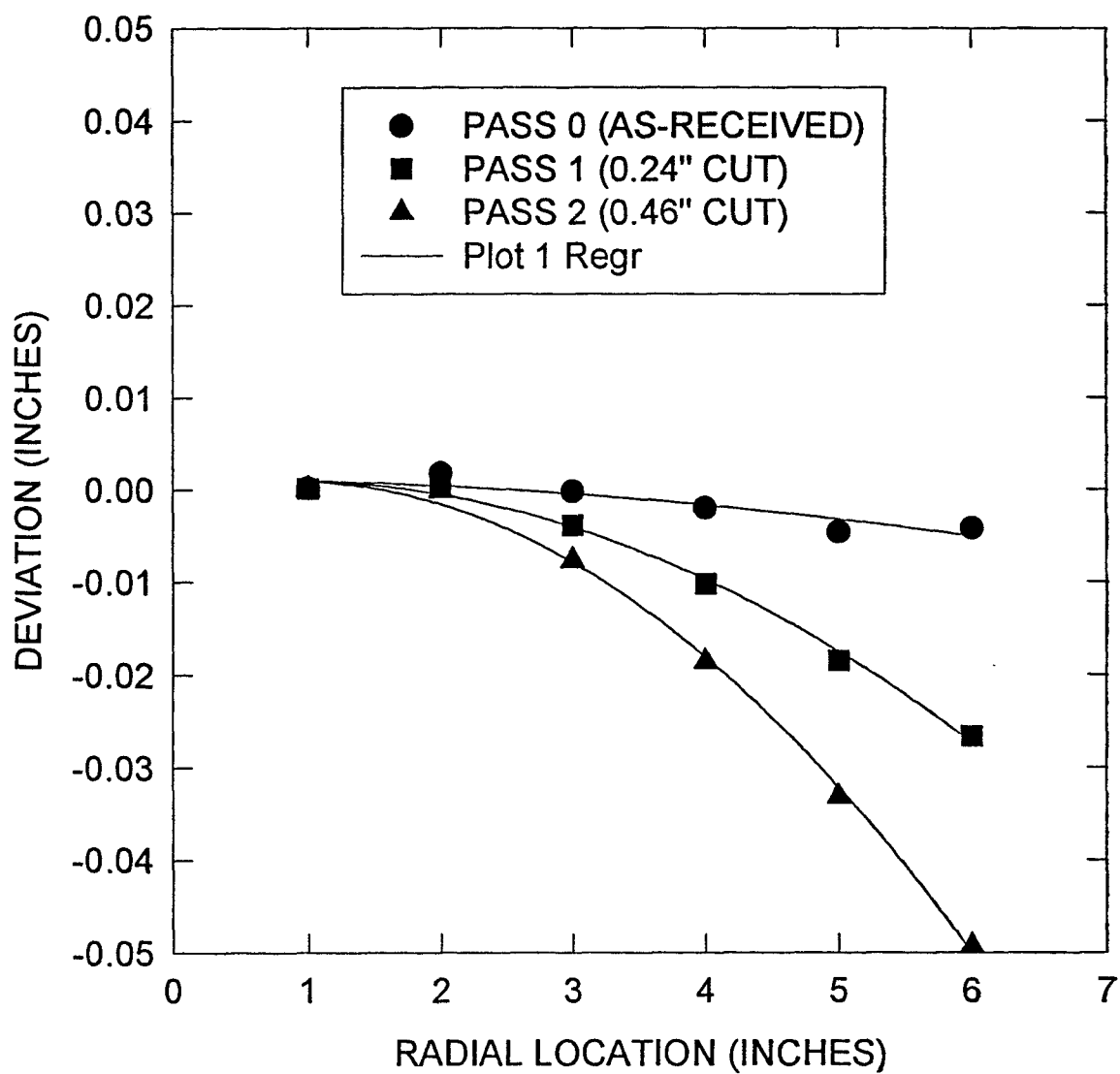
ANGLE	0	45	90	135	180	225	270	315	AVERAGE
				PART 3 RUN 1					
RADIAL 1	0.0021	0.0026	0.0009	0.0002	0.0009	0.0011	0.0008	-0.0006	0.0010
RADIAL 2	0.0077	0.0083	0.0064	0.0043	0.0069	0.0059	0.0059	0.0009	0.0058
RADIAL 3	0.0123	0.0098	0.0086	0.0077	0.0075	0.0075	0.0095	0.0106	0.0092
RADIAL 4	0.0175	0.0116	0.0125	0.0126	0.0084	0.0093	0.0140	0.0187	0.0131
RADIAL 5	0.0240	0.0132	0.0166	0.0162	0.0090	0.0098	0.0176	0.0257	0.0165
RADIAL 6	0.0239	0.0087	0.0136	0.0531	0.0041	0.0045	0.0151	0.0249	0.0185
NOTE: 12 O'CLOCK @ ANGLE=0 (CCW PROGRESSION)							R.ANG	THICK	
RADIAL 1 @ 1.1" RADIAL 2 THRU 6 @ 2" THRU 6"							6.000	1.918	
RUN 1=AS-RECEIVED							6.090	1.918	
							6.180	1.917	
							6.270	1.922	

ANGLE	0	45	90	135	180	225	270	315	AVERAGE
					PART 3 RUN 2				
RADIAL 1	0.0022	0.0035	0.0024	0.0017	0.0022	0.0015	-0.0001	-0.0010	0.0016
RADIAL 2	0.0066	0.0087	0.0079	0.0062	0.0080	0.0056	0.0043	-0.0011	0.0058
RADIAL 3	0.0083	0.0081	0.0088	0.0082	0.0069	0.0045	0.0048	0.0054	0.0069
RADIAL 4	0.0088	0.0060	0.0095	0.0101	0.0046	0.0023	0.0045	0.0081	0.0067
RADIAL 5	0.0091	0.0023	0.0084	0.0092	0.0003	-0.0028	0.0014	0.0085	0.0046
RADIAL 6	0.0013	-0.0091	0.0000	0.0400	-0.0110	-0.0152	-0.0088	-0.0006	-0.0004
							R.ANG	THICK	
NOTE: 12 O'CLOCK @ ANGLE=0 (CCW PROGRESSION)							6.000	1.693	
RADIAL 1 @ 1.1" RADIAL 2 THRU 6 @ 2" THRU 6"							6.090	1.699	
RUN 2=0.2" NOMINAL CUT							6.180	1.692	
							6.270	1.685	

ANGLE	0	45	90	PART 3 RUN 3 135	180	225	270	315	AVERAGE
RADIAL 1	0.0022	0.0034	0.0020	0.0011	0.0013	0.0010	0.0002	-0.0010	0.0013
RADIAL 2	0.0063	0.0082	0.0069	0.0047	0.0061	0.0040	0.0035	-0.0015	0.0048
RADIAL 3	0.0054	0.0047	0.0048	0.0035	0.0017	0.0001	0.0011	0.0023	0.0030
RADIAL 4	0.0008	-0.0025	0.0003	-0.0002	-0.0063	-0.0075	-0.0042	-0.0001	-0.0025
RADIAL 5	-0.0061	-0.0133	-0.0082	-0.0083	-0.0178	-0.0200	-0.0143	-0.0067	-0.0118
RADIAL 6	-0.0232	-0.0339	-0.0255	0.0129	-0.0391	-0.0422	-0.0344	-0.0252	-0.0263
NOTE: 12 O'CLOCK @ ANGLE=0 (CCW PROGRESSION)							R.ANG	THICK	
RADIAL 1 @ 1.1" RADIAL 2 THRU 6 @ 2" THRU 6"							6.000	1.444	
RUN 3=0.4" NOMINAL CUT							6.090	1.448	
							6.180	1.434	
							6.270	1.427	

WARPAGE MAP
PART 3
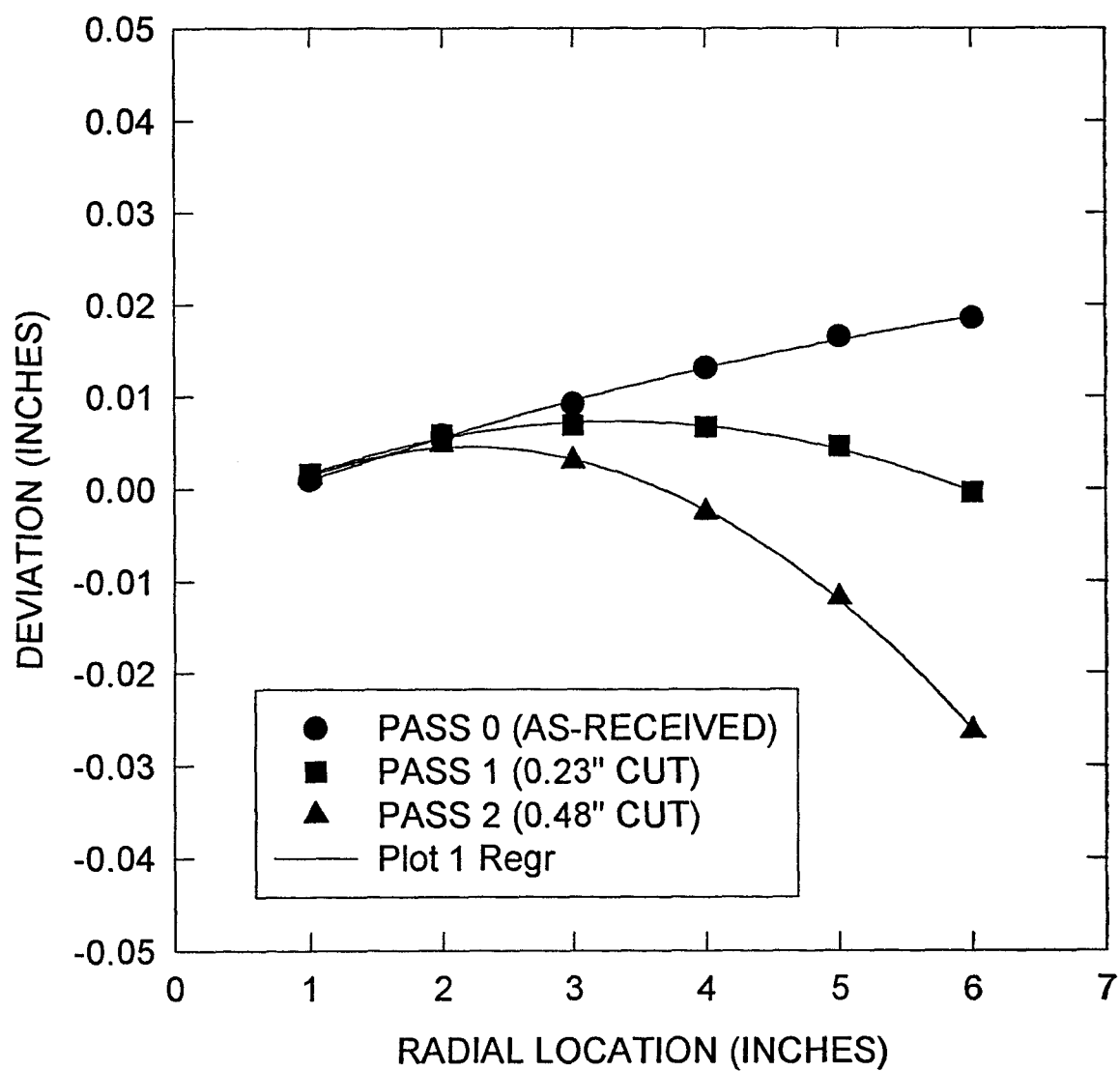
ANGLE	0	45	90	135	180	225	270	315	AVERAGE
					PART 4 RUN 1				
RADIAL 1	0.0006	0.0013	0.0016	0.0002	-0.0003	0.0004	0.0006	0.0007	0.0006
RADIAL 2	0.0022	0.0030	0.0053	-0.0002	-0.0008	0.0016	0.0020	0.0014	0.0018
RADIAL 3	-0.0003	0.0100	0.0081	-0.0057	-0.0061	0.0000	-0.0019	-0.0042	0.0000
RADIAL 4	-0.0043	0.0161	0.0112	-0.0138	-0.0123	-0.0021	-0.0054	-0.0103	-0.0026
RADIAL 5	-0.0103	0.0210	0.0135	-0.0225	-0.0185	-0.0025	-0.0094	-0.0164	-0.0056
RADIAL 6	-0.0225	0.0223	0.0127	0.0019	-0.0293	-0.0088	-0.0185	-0.0279	-0.0088
NOTE: 12 O'CLOCK @ ANGLE=0 (CCW PROGRESSION)							R.ANG	THICK	
RADIAL 1 @ 1.1" RADIAL 2 THRU 6 @ 2" THRU 6"							6.000	1.927	
RUN 1=AS-RECEIVED							6.090	1.928	
							6.180	1.929	
							6.270	1.934	

ANGLE	0	45	90	PART 4 RUN 2		225	270	315	AVERAGE
				135	180				
RADIAL 1	0.0007	0.0016	0.0018	0.0001	-0.0007	-0.0002	0.0003	0.0007	0.0005
RADIAL 2	0.0024	0.0035	0.0054	-0.0003	-0.0019	0.0004	0.0011	0.0013	0.0015
RADIAL 3	-0.0002	0.0103	0.0080	-0.0065	-0.0081	-0.0024	-0.0036	-0.0050	-0.0009
RADIAL 4	-0.0048	0.0160	0.0104	-0.0155	-0.0154	-0.0058	-0.0085	-0.0118	-0.0044
RADIAL 5	-0.0116	0.0198	0.0116	-0.0256	-0.0234	-0.0082	-0.0141	-0.0195	-0.0089
RADIAL 6	-0.0252	0.0200	0.0094	-0.0033	-0.0363	-0.0165	-0.0251	-0.0323	-0.0137
NOTE: 12 O'CLOCK @ ANGLE=0 (CCW PROGRESSION)							R.ANG	THICK	
RADIAL 1 @ 1.1" RADIAL 2 THRU 6 @ 2" THRU 6"							6.000	1.662	
RUN 2=0.2" NOMINAL CUT							6.090	1.669	
							6.180	1.635	
							6.270	1.660	

ANGLE	0	45	90	PART 4 RUN 3 135	180	225	270	315	AVERAGE
RADIAL 1	0.0005	0.0012	0.0016	0.0003	-0.0003	0.0004	0.0007	0.0008	0.0007
RADIAL 2	0.0019	0.0024	0.0047	-0.0006	-0.0014	0.0012	0.0017	0.0013	0.0014
RADIAL 3	-0.0017	0.0082	0.0061	-0.0075	-0.0080	-0.0017	-0.0033	-0.0056	-0.0017
RADIAL 4	-0.0076	0.0124	0.0071	-0.0176	-0.0161	-0.0058	-0.0089	-0.0134	-0.0062
RADIAL 5	-0.0162	0.0145	0.0066	-0.0290	-0.0250	-0.0089	-0.0154	-0.0223	-0.0120
RADIAL 6	-0.0320	0.0122	0.0022	-0.0083	-0.0394	-0.0185	-0.0278	-0.0369	-0.0186
NOTE: 12 O'CLOCK @ ANGLE=0 (CCW PROGRESSION)							R.ANG	THICK	
RADIAL 1 @ 1.1" RADIAL 2 THRU 6 @ 2" THRU 6"							6.000	1.440	
RUN 3=0.4" NOMINAL CUT							6.090	1.478	
							6.180	1.460	
							6.270	1.453	

WARPAGE MAP
PART 4
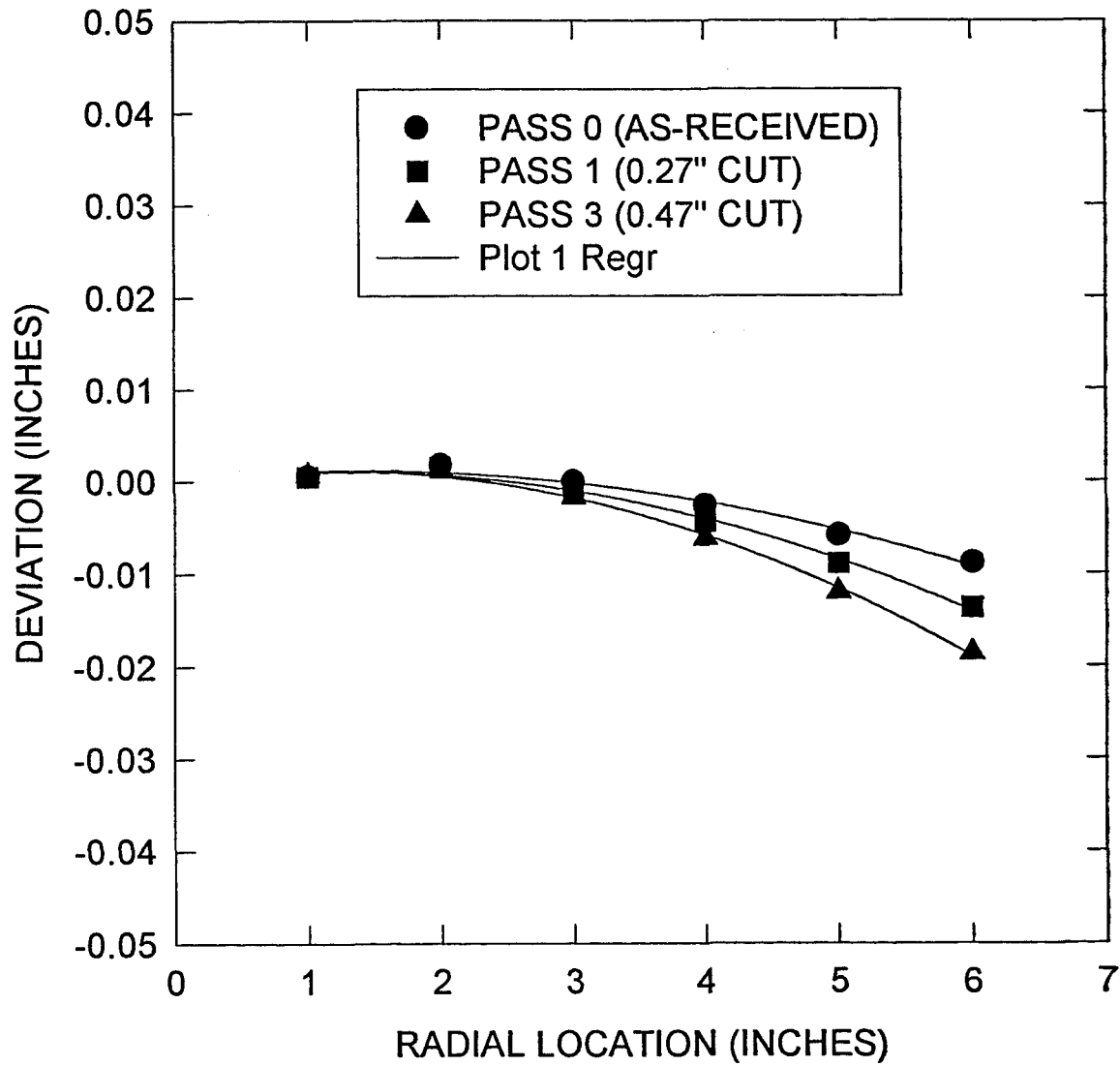
REPORT DOCUMENTATION PAGE

Public reporting burden for this collection of information is estimated to average 1 hour per response, including the time for reviewing instructions, searching existing data sources, gathering and maintaining the data needed, and completing and reviewing the collection of information. Send comments regarding this burden estimate or any other aspect of this collection of information, including suggestions for reducing this burden, to Washington Headquarters Services, Directorate for Information Operations and Reports, 1215 Jefferson Davis Highway, Suite 1204, Arlington, VA 22202-4302, and to the Office of Management and Budget, Paperwork Reduction Project (0704-0188), Washington, DC 20503.

1. AGENCY USE ONLY (*Leave blank*)	2. REPORT DATE	3. REPORT TYPE AND DATES COVERED
	January 2001	Technical Memorandum

4. TITLE AND SUBTITLE

The Effect of Heat Treatment on Residual Stress and Machining Distortions in Advanced Nickel Base Disk Alloys

6. AUTHOR(S)

John Gayda

5. FUNDING NUMBERS

WU–714–04–10–00

7. PERFORMING ORGANIZATION NAME(S) AND ADDRESS(ES)

National Aeronautics and Space Administration
John H. Glenn Research Center at Lewis Field
Cleveland, Ohio 44135–3191

8. PERFORMING ORGANIZATION REPORT NUMBER

E–12670

9. SPONSORING/MONITORING AGENCY NAME(S) AND ADDRESS(ES)

National Aeronautics and Space Administration
Washington, DC 20546–0001

10. SPONSORING/MONITORING AGENCY REPORT NUMBER

NASA TM—2001-210717

11. SUPPLEMENTARY NOTES

Responsible person, John Gayda, organization code 5120, 216–433–3273

12a. DISTRIBUTION/AVAILABILITY STATEMENT

Unclassified - Unlimited
Subject Category: 26   Distribution: Nonstandard

Available electronically at http://gltrs.grc.nasa.gov/GLTRS

This publication is available from the NASA Center for AeroSpace Information, 301–621–0390.

12b. DISTRIBUTION CODE

13. ABSTRACT *(Maximum 200 words)*

This paper describes an extension of NASA's AST and IDPAT Programs which sought to predict the effect of stabilization heat treatments on residual stress and subsequent machining distortions in the advanced disk alloy, ME-209. Simple "pancake" forgings of ME-209 were produced and given four heat treats: 2075F(SUBSOLVUS)/OIL QUENCH/NO AGE; 2075F/OIL QUENCH/1400F@8HR; 2075F/OIL QUENCH/1550F@3HR/1400F@8HR; and 2160F(SUPERSOLVUS)/ OIL QUENCH/1550F@3HR/1400F@8HR. The forgings were then measured to obtain surface profiles in the heat treated condition. A simple machining plan consisting of face cuts from the top surface followed by measurements of the surface profile opposite the cut were made. This data provided warpage maps which were compared with analytical results. The analysis followed the IDPAT methodology and utilized a 2-D axisymmetric, viscoplastic FEA code. The analytical results accurately tracked the experimental data for each of the four heat treatments. The 1550F stabilization heat treatment was found to significantly reduce residual stresses and subsequent machining distortions for fine grain (subsolvus) ME209, while coarse grain (supersolvus) ME209 would require additional time or higher stabilization temperatures to attain the same degree of stress relief.

14. SUBJECT TERMS

Superalloys; Disks; Residual stress

15. NUMBER OF PAGES

56

16. PRICE CODE

A04

17. SECURITY CLASSIFICATION OF REPORT	18. SECURITY CLASSIFICATION OF THIS PAGE	19. SECURITY CLASSIFICATION OF ABSTRACT	20. LIMITATION OF ABSTRACT
Unclassified	Unclassified	Unclassified	

NSN 7540-01-280-5500

Standard Form 298 (Rev. 2-89)
Prescribed by ANSI Std. Z39-18
298-102